NASA TECHNICAL NOTE

NASA TN D-2754

ℓ 1

NASA TN D-2754

ANALYTICAL STUDY OF EFFECTS
OF PRODUCT OF INERTIA ON
AIRPLANE SPIN ENTRIES,
DEVELOPED SPINS,
AND SPIN RECOVERIES

by Ernie L. Anglin

Langley Research Center
Langley Station, Hampton, Va.

NATIONAL AERONAUTICS AND SPACE ADMINISTRATION • WASHINGTON, D. C. • APRIL 1965

NASA TN D-2754

ANALYTICAL STUDY OF EFFECTS OF PRODUCT OF INERTIA

ON AIRPLANE SPIN ENTRIES, DEVELOPED SPINS,

AND SPIN RECOVERIES

By Ernie L. Anglin

Langley Research Center
Langley Station, Hampton, Va.

NATIONAL AERONAUTICS AND SPACE ADMINISTRATION

ANALYTICAL STUDY OF EFFECTS OF PRODUCT OF INERTIA

ON AIRPLANE SPIN ENTRIES, DEVELOPED SPINS,

AND SPIN RECOVERIES

By Ernie L. Anglin
Langley Research Center

SUMMARY

An analytical study has been made to investigate the effects of variations in product of inertia on the spin entry, developed spin, and spin recovery of airplanes. Three configurations considered to be representative of modern fighter-type airplanes were used: a delta-wing fighter, a swept-wing fighter, and a stub-wing research vehicle. They were mass loaded relatively heavily along the fuselage.

The results indicate that the magnitude of the product of inertia may have a significant effect on attempted spin-entry motions. For the delta-wing fighter and the swept-wing fighter, an increase in product of inertia changed the attempted entry motion from one in which a developed spin was attained to one in which no spin resulted. For developed spins, increasing the product of inertia caused slightly higher angles of attack, somewhat lower rates of rotation, and lower magnitudes of spin-energy factor resulting in fewer turns required for recovery. When spins are oscillatory, the trends noted for developed spins are somewhat obscured.

INTRODUCTION

It has long been recognized (for example, see refs. 1 and 2) that moment-of-inertia variations have large effects on developed-spin and recovery motions of airplanes and that these motions are particularly affected by whether the vehicle is mass loaded more heavily along its fuselage or its wing and by the degree of difference between the wing and fuselage loading. Results of reference 1 show that this difference in wing and fuselage loadings is extremely important both in algebraic sign and in magnitude. No information exists, however, with regard to possible effects of product-of-inertia variations due to varying displacements of the principal longitudinal axis with respect to the fuselage reference (body) axis of the airplane.

The present investigation was therefore made to determine analytically the effects of product-of-inertia variations on the spin-entry, developed-spin, and

spin-recovery motions. The product-of-inertia variations used correspond to angular displacements between the reference and principal axes from 0° to 5°. Three representative modern airplane configurations mass loaded relatively heavily along the fuselage were used: a delta-wing fighter, a swept-wing fighter, and a stub-wing research vehicle. A high-speed digital computer, wind-tunnel aerodynamic data, six-degree-of-freedom equations of motion, and methods similar to those used in references 3, 4, and 5 were utilized to calculate the airplane motions.

SYMBOLS

The body system of axes was used in the calculations. This system of axes, related angles, and positive directions of corresponding forces and moments are illustrated in figure 1.

b   wing span, ft

C_l rolling-moment coefficient, $\dfrac{M_X}{\frac{1}{2}\rho V_R^2 Sb}$

C_m pitching-moment coefficient, $\dfrac{M_Y}{\frac{1}{2}\rho V_R^2 S\bar{c}}$

C_n yawing-moment coefficient, $\dfrac{M_Z}{\frac{1}{2}\rho V_R^2 Sb}$

C_X longitudinal-force coefficient, $\dfrac{F_X}{\frac{1}{2}\rho V_R^2 S}$

C_Y side-force coefficient, $\dfrac{F_Y}{\frac{1}{2}\rho V_R^2 S}$

C_Z normal-force coefficient, $\dfrac{F_Z}{\frac{1}{2}\rho V_R^2 S}$

$$C_{l_p} = \frac{\partial C_l}{\partial\left(\dfrac{pb}{2V_R}\right)}$$

$$C_{l_r} = \frac{\partial C_l}{\partial \left(\frac{rb}{2V_R}\right)}$$

$$C_{l_\beta} = \frac{\partial C_l}{\partial \beta}$$

$C_{l_{\delta_a}}$ rolling-moment coefficient due to aileron deflection, per deg

$C_{l_{\delta_r}}$ rolling-moment coefficient due to rudder deflection, per deg

$$C_{m_q} = \frac{\partial C_m}{\partial \left(\frac{q\bar{c}}{2V_R}\right)}$$

$$C_{m_{\dot{\alpha}}} = \frac{\partial C_m}{\partial \left(\frac{\dot{\alpha}\bar{c}}{2V_R}\right)}$$

$C_{m_{\delta_e}}$ pitching-moment coefficient due to elevator deflection, per deg

$$C_{n_p} = \frac{\partial C_n}{\partial \left(\frac{pb}{2V_R}\right)}$$

$$C_{n_r} = \frac{\partial C_n}{\partial \left(\frac{rb}{2V_R}\right)}$$

$$C_{n_\beta} = \frac{\partial C_n}{\partial \beta}$$

$C_{n_{\delta_a}}$ yawing-moment coefficient due to aileron deflection, per deg

$C_{n_{\delta_r}}$ yawing-moment coefficient due to rudder deflection, per deg

$C_{X_{\delta_e}}$ longitudinal-force coefficient due to elevator deflection,
        per deg

$$C_{Y_\beta} = \frac{\partial C_Y}{\partial \beta}$$

$C_{Y_{\delta_a}}$ side-force coefficient due to aileron deflection, per deg

$C_{Y_{\delta_r}}$ side-force coefficient due to rudder deflection, per deg

$C_{Z_{\delta_e}}$ normal-force coefficient due to elevator deflection, per deg

$\bar{c}$ mean aerodynamic chord, ft

E_s nondimensional spin energy factor, $\dfrac{\frac{1}{2} I_V \dot{\psi}_e^2}{\frac{1}{2} \rho V_R^2 Sb}$

F_X longitudinal force acting along X-axis, lb

F_Y side force acting along Y-axis, lb

F_Z normal force acting along Z-axis, lb

g acceleration due to gravity, 32.17 ft/sec^2

h altitude, ft

h_0 initial altitude, ft

I_V moment of inertia about vertical axis, slug-ft^2

$I_{X_0}, I_{Y_0}, I_{Z_0}$ moment of inertia about X_0-, Y_0-, and Z_0-axis, respectively, slug-ft^2

I_X, I_Y, I_Z moment of inertia about X-, Y-, and Z-axis, respectively, slug-ft^2

I_{XZ} product of inertia in XZ-plane, positive when X_0-axis is inclined below X-axis at nose, slug-ft^2

$\dfrac{I_X - I_Y}{mb^2}$ inertia yawing-moment parameter

M_X rolling moment acting about X-axis, ft-lb

M_Y	pitching moment acting about Y-axis, ft-lb
M_Z	yawing moment acting about Z-axis, ft-lb
m	mass, W/g, slugs
p,q,r	component of resultant angular velocity about X-, Y-, and Z-axis, respectively, rad/sec
S	wing area, sq ft
t	time, sec
u,v,w	component of resultant linear velocity V_R along X-, Y-, and Z-axis, respectively, ft/sec
V_R	resultant linear velocity, ft/sec
W	weight, lb
X,Y,Z	body axes
X_0,Y_0,Z_0	principal axes (axes about which the products of inertia are zero)
α	angle of attack, angle between relative wind V_R projected into XZ-plane of symmetry and X-axis, positive when relative wind comes from below XY-plane, deg
β	angle of sideslip, angle between relative wind V_R and projection of relative wind on XZ-plane, positive when relative wind comes from right of plane of symmetry, deg
δ_a	aileron deflection with respect to chord line of wing, positive when trailing edge of right aileron down (left stick), deg
δ_e	elevator deflection with respect to fuselage reference line, positive with trailing edge down, deg
δ_r	rudder deflection with respect to fin, positive when trailing edge left, deg
ϵ	angle between X-axis and X_0-axis, positive when principal axis is below reference axis at nose, deg
θ_e	total angular movement of X-axis from horizontal plane measured in vertical plane, positive when airplane nose is above horizontal plane, rad or deg

ρ air density, slugs/cu ft

ϕ angle between Y-axis and horizontal measured in vertical plane, positive for erect spins when right wing downward and for inverted spins when left wing downward, rad or deg

ϕ_e total angular movement of Y-axis from horizontal plane measured in YZ-plane, positive when clockwise as viewed from rear of airplane (if X-axis is vertical, ϕ_e is measured from a reference position in horizontal plane), rad or deg

ψ_e horizontal component of angular deflection of X-axis from reference position in horizontal plane, positive when clockwise as viewed from vertically above airplane, rad or deg

A dot over a symbol represents a derivative with respect to time; for example, $\dot{u} = du/dt$.

METHODS AND CALCULATIONS

The spin-entry attempts and the developed-spin and spin-recovery motions were calculated by using a high-speed digital computer which solved the equations of motion and associated formulas listed in the appendix. The equations of motion represent six degrees of freedom along and about the body system of axes. (See fig. 1 for illustration of body axes.)

Sketches of the planforms of the three configurations used in the study are shown in figure 2. Configuration A represents a delta-wing fighter, configuration B represents a swept-wing fighter, and configuration C represents a stub-wing research vehicle. The mass and dimensional characteristics of these configurations are listed in table I.

The aerodynamic data inputs used in the digital computer calculations are presented in figures 3 to 8. The data for configurations A, B, and C were obtained from references 4, 6, and 3, respectively. Estimated values of the derivatives C_{m_q} and $C_{m_{\dot{\alpha}}}$ were used in the pitching equation of motion (see appendix) and were constant for all angles of attack. Values of C_{m_q} and $C_{m_{\dot{\alpha}}}$ were -0.45 and -0.45 for configuration A (ref. 4) and -10.0 and 0 for configuration C (ref. 3). Values of C_{m_q} and $C_{m_{\dot{\alpha}}}$ used for configuration B in this investigation were estimated to be -2.0 and 0, respectively. No values of the derivatives C_{l_r} and C_{n_p} for configurations B and C were available and for purposes of this study they were assumed to be 0.

The procedure for calculating attempted spin entries was as follows: The configuration initially was in trimmed level flight. At zero time, the elevator was deflected full up from its trimmed level flight position. As the motion developed, rudder and aileron controls were applied at times conducive to the

attaining and sustaining of a developed right spin (turning toward the pilot's right). The initial conditions used for these calculations are shown in table II.

Developed spins were obtained in a manner similar to the spin-tunnel testing technique. (See ref. 4.) In this method, it is assumed that the initial condition is one of very high angle of attack with applied rotation about a vertical axis and that from this condition the spin parameters will undergo some intermediate motions until the configuration eventually achieves its own equilibrium-developed spin. The initial conditions used for these calculations are included in table II.

Spin-recovery attempts were made by deflecting the rudder against the direction of rotation and by deflecting the ailerons with the direction of roll (left rudder and right ailerons when in an erect spin to the pilot's right); these are the optimum control deflections for recovery from developed spins for airplanes loaded relatively heavily along the fuselage (ref. 1), as are the configurations investigated herein. The elevators remained in the original elevator-up setting. A spin is considered terminated when either the spin rotation ceases or the angle of attack becomes and remains less than the stall angle. Usually when the angle of attack becomes less than the stall angle, the airplane enters a steep dive without significant rotation ($\dot{\psi}_e \approx 0$). In some instances, however, the airplane may be turning or rolling in a spiral glide or an aileron roll. Also, sometimes the airplane may roll or pitch to an inverted attitude from the erect spin and may still have some rotation, but it is considered to be out of the original erect spin.

The product-of-inertia variations were assumed to be due to weight shifts inside the aircraft, accomplished in such a manner as to cause angular displacements of the X_0-axis (principal axis) below the reference X-axis (body axis) at angles ranging from $0°$ to $5°$. The equations used to obtain values for the moments and product of inertia about the body axes are from reference 7 and are as follows:

$$I_X = \frac{1}{2}\left(I_{Z_0} + I_{X_0}\right) - \frac{1}{2}\left(I_{Z_0} - I_{X_0}\right)\cos 2\epsilon$$

$$I_Y = I_{Y_0}$$

$$I_Z = \frac{1}{2}\left(I_{Z_0} + I_{X_0}\right) + \frac{1}{2}\left(I_{Z_0} - I_{X_0}\right)\cos 2\epsilon$$

$$I_{XZ} = \frac{1}{2}\left(I_{Z_0} - I_{X_0}\right)\sin 2\epsilon$$

The moments and product of inertia obtained from these equations for each configuration are presented in table III as a function of ϵ. In addition, values of the inertia yawing-moment parameter $\dfrac{I_X - I_Y}{mb^2}$ for each configuration are

7

given in table III. Changes in the algebraic sign or large changes in the magnitude of this parameter may have an important influence not only on the developed spin characteristics but also on the particular combination of controls which are considered to be the optimum controls for recovery (ref. 1). The variations in yawing-moment parameter shown in table III are not of a large enough magnitude to be important.

RESULTS AND DISCUSSION

Results of the calculations of the spin-entry, developed-spin, and spin-recovery motions for $\epsilon = 0°$ and $\epsilon = 5°$ are presented in figures 9 to 14 as time histories of angle of attack, angle of pitch, sideslip angle, roll attitude, rate of spin rotation, number of spinning turns made, and aileron- and rudder-control inputs. Some pertinent results from the developed-spin and spin-recovery calculations are also presented in table IV for values of ϵ from $0°$ to $5°$ in $1°$ increments.

Spin-Entry Calculations

Spin-entry attempts were calculated for each configuration for values of ϵ of $0°$ and $5°$ only. Therefore, only overall effects were obtained — in particular, whether the variation in magnitude of product of inertia used would change the attempted entry motion from one in which a developed spin was attained to one in which no spin resulted. The same initial conditions and control movements were used for both the $\epsilon = 0°$ and the $\epsilon = 5°$ calculations for each model.

Configuration A.- The results of the spin-entry calculations for configuration A are presented in figure 9. For $\epsilon = 0°$ $\left(I_{XZ} = 0 \text{ slug-ft}^2\right)$, a spin-entry motion occurred in which two turns were made in the first 27 seconds. The angle of attack increased smoothly upward with oscillations steadily decreasing in amplitude, and the configuration apparently was headed toward an equilibrium developed spin condition with an angle of attack above $60°$ and with a rate of spin rotation $\dot{\psi}_e$ of less than 1 radian per second.

For $\epsilon = 5°$ $\left(I_{XZ} = 10\ 827 \text{ slug-ft}^2\right)$, the angle-of-attack curve shows two oscillations which were approximately the same as those obtained for $\epsilon = 0°$. After that, however, the angle of attack for $\epsilon = 5°$ increased very rapidly until it went above $120°$ and beyond the aerodynamic data range used in this study. At the same time, θ_e and β were changing violently and $\dot{\psi}_e$ did not appear to be headed toward any positive equilibrium value. Although the motion did not show beyond question that this is a no-spin condition, past experience indicates that an airplane normally would not enter a spin after having gone through such gyrations.

Configuration B.- The results of the spin-entry calculations for configuration B are presented in figure 10. For $\epsilon = 0°$ the motion was oscillatory and a rollover occurred after approximately 10 to 11 seconds, after which an erect

developed spin was obtained. The angle-of-attack curves for $\epsilon = 0^\circ$ and $\epsilon = 5^\circ$ coincide for the first two oscillations, after which oscillations for $\epsilon = 5^\circ$ occurred about a much lower angle of attack. Finally, the angle of attack became negative; this indicates a no-spin condition.

Configuration C.- The results of the spin-entry calculations for configuration C are presented in figure 11. Spins were obtained with angles of attack greater than 80° for both $\epsilon = 0^\circ$ and $\epsilon = 5^\circ$, and increasing ϵ had little or no effect on the entry motions. The spin entry did progress slightly faster for $\epsilon = 0^\circ$, however, inasmuch as two turns were achieved at 31 seconds compared with 34 seconds for $\epsilon = 5^\circ$.

Summary of entry results.- A variation of 5° in the displacement of the X_0-axis (principal axis) below the reference X-axis (body axis) may have a significant effect on attempted spin entries. In general, an increase in ϵ appeared to increase the degree of the oscillations occurring during the post-stall gyrations. Sometimes these increases in oscillations may lessen the tendency of a given configuration to enter a spin.

The time histories of configuration C show very mild oscillations when compared with those obtained for configurations A and B. (Compare fig. 11 with figs. 9 and 10.) An examination of the equations of motion (see appendix) indicates that the magnitude of the effect produced by the product of inertia I_{XZ} depends on the magnitudes of p, q, and r. A larger effect would therefore be expected on motions which are more oscillatory.

Developed-Spin Calculations

The results of the developed-spin calculations are presented in table IV for configurations A, B, and C for values of ϵ of 0°, 1°, 2°, 3°, 4°, and 5°. The same control settings and initial conditions were used for all values of ϵ for each configuration. The calculations for each configuration allowed time for any disturbance caused by the specific combinations of initial conditions used to damp out and for the configuration to achieve its own equilibrium developed spin. The spin parameters presented in table IV are for the equilibrium developed spins and are, therefore, the values present just prior to the application of the recovery controls. Recovery controls were then applied.

Configuration A.- The results of the developed-spin calculations for $\epsilon = 0^\circ$ and $\epsilon = 5^\circ$ for configuration A are presented in figure 12. With $\epsilon = 0^\circ$ (fig. 12(a)), configuration A had a very steady developed spin with an angle of attack of 74°, sideslip and roll angles near 0°, and a rotation rate of 1.26 radians per second. The results presented in table IV indicate the manner in which the developed-spin parameters are affected as ϵ was varied from 0° to 5°. A comparison of figures 12(a) and 12(b) (or the developed-spin results, for $\epsilon = 0^\circ$ and $\epsilon = 5^\circ$ shown in table IV) indicates that the steady nature of the developed spins was not affected by changes in ϵ. The angles of attack remained at approximately 74°, although table IV shows that a very slight increase occurred as ϵ increased, the sideslip and roll angles remained near 0°, and the rate of rotation decreased from 1.26 for $\epsilon = 0^\circ$ to 1.15 for $\epsilon = 5^\circ$.

Configuration B.- The results of the developed-spin calculations for configuration B are presented in figure 13. With $\epsilon = 0^\circ$, configuration B had an oscillatory developed spin. The angle of attack oscillated from 65° to 85°, the sideslip and roll angles oscillated from approximately -20° to 20°, and the rate of rotation varied from 1.69 to 2.63 radians per second.

An examination of the results presented in table IV indicates that as ϵ increased, the angle-of-attack oscillations increased, whereas the sideslip-angle and roll-angle oscillations decreased a few degrees. The average angle of attack remained at approximately 76°, although table IV shows that a very slight increase occurred as ϵ increased. However, the trend was not as consistent for configuration B as it was for configuration A. The average rate of rotation decreased from approximately 2.17 for $\epsilon = 0^\circ$ to 2.00 for $\epsilon = 5^\circ$, a trend similar to that noted for configuration A.

Configuration C.- The results of the developed-spin calculations for configuration C are presented in figure 14. For $\epsilon = 0^\circ$, configuration C had a relatively steady developed spin with an angle of attack of approximately 85° and a rate of rotation of 2.07 radians per second.

An examination of table IV indicates that the steady nature of the developed spin remained the same for all values of ϵ. The average angle of attack remained at approximately 85°, although table IV shows that a very slight increase occurred as ϵ increased. The rate of rotation decreased from 2.07 for $\epsilon = 0^\circ$ to 1.65 for $\epsilon = 5^\circ$.

Summary of developed-spin results.- A summary of the results of the developed-spin calculations is presented in figures 15 and 16 where the values of $\alpha_{average}$ and $\dot{\psi}_{e,average}$, respectively, are plotted as a function of ϵ. The average angle of attack (fig. 15) for each configuration remains approximately the same as ϵ increases. Very slight angle-of-attack increases did occur, but the magnitude of these increases is too small to be significant. The rate of rotation (fig. 16) for each configuration decreases as ϵ increases.

Analysis of developed-spin results.- The magnitude of the effect produced by product of inertia depends on the magnitudes of p, q, and r. In general, in a developed spin, the magnitudes of the oscillations and, therefore, the magnitudes of p, q, and r are not as great as those which occur during a spin-entry maneuver. Hence, the magnitude of the effect produced by a product of inertia would be expected to be less on a developed-spin motion than on a spin-entry motion.

The probable effect of product of inertia on the relative difficulty of spin recovery may be determined from the following analysis. Since the average angle of attack remained approximately the same when ϵ was increased, the decrease in $\dot{\psi}_e$ as ϵ was increased may be explained by an equation from reference 1. This equation, which approximates the rate of rotation of a vehicle in a developed spin, is

10

$$\dot{\psi}_e^{\,2} = \frac{-M_Y}{\frac{1}{2}\left(I_Z - I_X\right)\sin 2\alpha}$$

When this relationship is revised to include the product of inertia, it becomes

$$\dot{\psi}_e^{\,2} = \frac{-M_Y}{\frac{1}{2}\left(I_Z - I_X\right)\sin 2\alpha - I_{XZ}\cos 2\alpha}$$

Inasmuch as the average angle of attack remains approximately the same, the numerator of this expression remains approximately the same. However, as ϵ increases, the magnitude of the denominator increases for all developed spins having an angle of attack greater than 45° ($\alpha > 45^\circ$ for each of the configurations investigated herein); this increase causes a decrease in the value of $\dot{\psi}_e$.

Since the average angle of attack remains approximately the same as ϵ increases, the accompanying decrease in rotation rate becomes important. As was pointed out in references 1 and 5, the lower the rate of spin rotation, the more rapid the recovery should be. In reference 5, a nondimensional spin-energy factor E_s, based on the kinetic energy of spin rotation, was shown to indicate the relative difficulty of spin recovery. The equation used for calculating E_s in reference 5 revised for this investigation to include the product of inertia becomes

$$E_s = \frac{\frac{1}{2} I_V \dot{\psi}_e^{\,2}}{\frac{1}{2}\rho V_R^2 Sb}$$

where

$$I_V = I_X \cos^2\alpha + I_Z \sin^2\alpha - I_{XZ}\sin 2\alpha$$

Values of E_s were obtained for configurations A, B, and C by using the revised equations and are presented as a function of ϵ in figure 17. For all three configurations investigated, the magnitude of E_s generally decreased consistently as ϵ increased. The decreases in E_s for configuration A are small in terms of absolute values but are large in terms of percent change, and actually represent a significant reduction. This reduction is illustrated more effectively in figure 18 where the variation of $\dfrac{E_s}{E_s \text{ for } \epsilon = 0^\circ}$ with ϵ is presented. The values of E_s for $\epsilon = 5^\circ$ represent approximately 80, 81, and 64 percent of the E_s values obtained for $\epsilon = 0^\circ$ for configurations A, B, and C, respectively.

11

Spin-Recovery Calculations

Attempts were made to calculate the spin-recovery from each of the developed-spin calculations. The results of the spin-recovery calculations are included in figures 12 to 14 and table IV.

A summary of the calculated recovery results is presented in figure 19, in which turns for recovery are presented as a function of ϵ. The turns required for recovery for configurations A and C consistently decreased as ϵ increased. This decrease would be expected because the value of E_s decreased consistently as ϵ increased (fig. 18). The turns required for recovery for configuration B also show an overall decrease, but the trend was not as consistent as it was for configurations A and C.

Additional Calculations for Configuration B

Inasmuch as the turns required for recovery for configuration B did not show as consistent a trend with ϵ changes as was noted for configurations A and C and inasmuch as configuration B was the only configuration which had an oscillatory spin, some additional calculations were made in an attempt to obtain a less oscillatory developed spin and to reinvestigate the effects of changes in ϵ. In these calculations the estimated values of C_m and C_{l_β} shown in figure 20 were used, with all other aerodynamic data inputs unchanged.

The results of the additional developed-spin calculations for configuration B are presented in the time histories of figure 21 and in table V. For $\epsilon = 0°$, an oscillatory developed spin is still obtained, but the magnitude of the oscillations is greatly reduced (compare fig. 13(a) with fig. 21(a)).

The results shown in table V indicate that the oscillatory nature of the developed spin shown in figure 21(a) remained about the same for all values of ϵ. The average angle of attack remained at approximately $67°$ and the rate of rotation decreased as ϵ increased. A summary of these additional results for configuration B is presented in figure 22, in which $\alpha_{average}$, $\dot{\psi}_{e,average}$, E_s, and turns for recovery are plotted against ϵ. The magnitude of the spin-energy factor E_s again decreased consistently as ϵ increased. (The value of E_s for $\epsilon = 5°$ is only 85 percent of the value of E_s for $\epsilon = 0°$.) The turns for recovery also show an overall decrease as ϵ increases, with a more definite trend than that previously obtained when the developed spins were more oscillatory. (Compare turns for recovery for configuration B in figs. 19 and 22.) Therefore, it appears that the inconsistencies noted in figure 19 in the trends of the turns required for recovery for configuration B were caused by the more oscillatory nature of the spins from which those recoveries were obtained.

12

General Remarks

The magnitudes of improvement in the spin recoveries shown in tables IV and V probably can be achieved with similar configurations having mass distributions somewhat similar to those used in the present investigation. Any attempt to obtain these magnitudes of improvement by readjusting interior mass arrangements so as to achieve a larger angle between the X_0-axis (principal axis) and the reference X-axis (body axis), particularly angles as large as 5^0, would probably be impractical. However, the results presented herein do indicate that, if a choice exists, the mass distribution which has the largest product of inertia I_{XZ} will have the best developed-spin and spin-recovery characteristics. In addition, the mass distribution with the largest product of inertia will have a more oscillatory spin-entry motion which, in some instances, may lessen the tendency of a given configuration to enter a spin. This trend occurs even though the mass loading parameters which are customarily used to predict effects on spins and recoveries remain essentially unchanged.

In addition, studies made in the past to analyze the spin-entry, developed-spin, and spin-recovery characteristics of specific aircraft (refs. 3 and 8) have neglected the product-of-inertia term in the equations of motion. As indicated by the results presented herein, the product of inertia may have an important effect on spins and recoveries and it should therefore be considered in future analytical studies pertinent to investigating the spin-entry, developed-spin, and spin-recovery characteristics of specific aircraft.

CONCLUSIONS

An analytical study of the effects of variations in product of inertia on the spin-entry, developed-spin, and spin-recovery characteristics for a delta-wing fighter, a swept-wing fighter, and a stub-wing research vehicle with mass distributed relatively heavily along the fuselage indicates the following conclusions:

1. For a given mass-loading arrangement such as is customarily described in terms of moments of inertia referenced to the body axes, a product of inertia due to the angular displacement of the X_0-axis (principal axis) below the reference X-axis (body axis) may have important effects on the spin-entry, developed-spin, and spin-recovery motions and should be considered in investigations pertinent to analyzing these motions for specific aircraft.

2. In general, an increase in product of inertia appears to increase the degree of the oscillations occurring during a spin-entry motion. These increased oscillations in some instances may lessen the tendency of a given configuration to enter a spin. For example, for the delta-wing fighter and the swept-wing fighter, increasing the angular displacement of the X_0-axis by 5^0 changed the spin-entry motion from a spin entry to a no-spin condition.

3. Increasing product of inertia generally did not alter the steady or oscillatory nature of the developed spins. Increasing product of inertia,

however, did cause the developed spins to have slightly higher average angles of attack, lower rates of rotation, and lower magnitudes of spin-energy factor. Because of the lower spin-energy factors, fewer turns were required for spin recovery.

4. As the developed spins become more oscillatory, the effects of increasing product of inertia tend to become obscured.

Langley Research Center,
     National Aeronautics and Space Administration,
          Langley Station, Hampton, Va., January 7, 1965.

EQUATIONS OF MOTION AND ASSOCIATED FORMULAS

The following equations of motion were used in calculating the spinning motions:

$$\dot{p} = \frac{I_Y - I_Z}{I_X}\,qr + \frac{I_{XZ}}{I_X}(\dot{r} + pq) + \frac{\rho V_R^2 Sb}{2I_X}\left[C_{l_\beta}\beta + C_{l_{\delta_a}}\delta_a + C_{l_{\delta_r}}\delta_r + \frac{b}{2V_R}\left(C_{l_p}p + C_{l_r}r\right)\right]$$

$$\dot{q} = \frac{I_Z - I_X}{I_Y}\,pr + \frac{I_{XZ}}{I_Y}(r^2 - p^2) + \frac{\rho V_R^2 S\bar{c}}{2I_Y}\left[C_m + C_{m_{\delta_e}}\delta_e + \frac{\bar{c}}{2V_R}\left(C_{m_q}q + C_{m_{\dot\alpha}}\dot\alpha\right)\right]$$

$$\dot{r} = \frac{I_X - I_Y}{I_Z}\,pq + \frac{I_{XZ}}{I_Z}(\dot{p} - qr) + \frac{\rho V_R^2 Sb}{2I_Z}\left[C_{n_\beta}\beta + C_{n_{\delta_a}}\delta_a + C_{n_{\delta_r}}\delta_r + \frac{b}{2V_R}\left(C_{n_p}p + C_{n_r}r\right)\right]$$

$$\dot{u} = -g\sin\theta_e + vr - wq + \frac{\rho V_R^2 S}{2m}\left(C_X + C_{X_{\delta_e}}\delta_e\right)$$

$$\dot{v} = g\cos\theta_e \sin\phi_e + wp - ur + \frac{\rho V_R^2 S}{2m}\left(C_{Y_\beta}\beta + C_{Y_{\delta_a}}\delta_a + C_{Y_{\delta_r}}\delta_r\right)$$

$$\dot{w} = g\cos\theta_e \cos\phi_e + uq - vr + \frac{\rho V_R^2 S}{2m}\left(C_Z + C_{Z_{\delta_e}}\delta_e\right)$$

In addition, the following auxiliary formulas were used:

$$\alpha = \tan^{-1}\frac{w}{u}$$

$$\beta = \sin^{-1}\frac{v}{V_R}$$

$$V_R = \sqrt{u^2 + v^2 + w^2}$$

$$\dot{h} = u \sin \theta_e - v \cos \theta_e \sin \phi_e - w \cos \theta_e \cos \phi_e$$

$$h = h_0 + \int \dot{h}\ dt$$

$$\dot{\theta}_e = q \cos \phi_e - r \sin \phi_e$$

$$\dot{\phi}_e = p + r \tan \theta_e \cos \phi_e + q \tan \theta_e \sin \phi_e$$

$$\dot{\psi}_e = \frac{\dot{\phi}_e - p}{\sin \theta_e}$$

$$\phi = \sin^{-1}\left(\sin \phi_e \cos \theta_e\right)$$

$$\text{Turns in spin} = \frac{\int \dot{\psi}_e\ dt}{2\pi}$$

REFERENCES

1. Neihouse, Anshal I.; Klinar, Walter J.; and Scher, Stanley H.: Status of Spin Research for Recent Airplane Designs. NASA TR R-57, 1960. (Supersedes NACA RM L57F12.)

2. Neihouse, Anshal I.: The Effect of Variations in Moments of Inertia on Spin and Recovery Characteristics of a Single-Engine Low-Wing Monoplane With Various Tail Arrangements, Including a Twin Tail. NACA TN 1575, 1948.

3. Grantham, William D.; and Scher, Stanley H.: Analytical Investigation and Prediction of Spin and Recovery Characteristics of the North American X-15 Airplane. NASA TM X-294, 1960.

4. Scher, Stanley H.; Anglin, Ernie L.; and Lawrence, George F.: Analytical Investigation of Effect of Spin Entry Technique on Spin and Recovery Characteristics for a 60° Delta-Wing Airplane. NASA TN D-156, 1959.

5. Anglin, Ernie L.; and Scher, Stanley H.: Analytical Study of Aircraft-Developed Spins and Determination of Moments Required for Satisfactory Spin Recovery. NASA TN D-2181, 1964.

6. Hewes, Donald E.: Low-Subsonic Measurements of the Static and Oscillatory Lateral Stability Derivatives of a Sweptback-Wing Airplane Configuration at Angles of Attack From -10° to 90°. NASA MEMO 5-20-59L, 1959.

7. Wolowicz, Chester H.; and Holleman, Euclid C.: Stability-Derivative Determination From Flight Data. AGARD Rep. 224, Oct. 1958.

8. Grantham, William D.: Analytical Investigation of the Spin and Recovery Characteristics of a Supersonic Trainer Airplane Having a 24° Swept Wing. NASA TM X-606, 1962.

TABLE I.- MASS AND DIMENSIONAL CHARACTERISTICS

	Configuration A	Configuration B	Configuration C
W, lb	24 811	23 771	12 575
S, sq ft	695.05	385.33	200
b, ft	38.12	35.67	22.36
$\bar{c}$, ft	23.755	11.83	10.27
Center of gravity, percent $\bar{c}$	30.0	33.0	19.5
I_{X_0}, slug-ft^2	13 449	11 709	4 288
I_{Y_0}, slug-ft^2	128 000	82 654	73 384
I_{Z_0}, slug-ft^2	138 151	89 237	74 867
$\dfrac{I_X - I_Y}{mb^2}$	$-1\ 022 \times 10^{-4}$	-825×10^{-4}	$-3\ 536 \times 10^{-4}$
δ_e, deg	-25	-30	-30
δ_r, deg	±25	±6	$\pm 7\frac{1}{2}$
δ_a, deg	±7	±15	$\pm 7\frac{1}{2}$

TABLE II.- INITIAL CONDITIONS USED IN CALCULATIONS

	Configuration A		Configuration B			Configuration C	
	Spin-entry attempts	Developed spins	Spin-entry attempts	Developed spins	Additional developed spins	Spin-entry attempts	Developed spins
α, deg	18	70.1	10	85	66.28	25	55
β, deg	0	-0.3	0	0	-2.85	0	-2
θ_e, deg	18	-19.9	10	-5	-23.72	25	-35
ϕ_e, deg	0	0	0	0	0	0	0
V_R, ft/sec	409.27	324.7	702.15	339.66	363.52	365.95	319.22
$\dot{\psi}_e$, rad/sec	0	1.07	0	2.5	1.24	0	0.45
h, ft	40 000	40 000	40 000	40 000	40 000	40 000	40 000
δ_e, deg	-25	-25	-30	-30	-20	-30	-30
δ_r, deg	0	25 right	0	6 right	6 right	0	7.5 right
δ_a, deg	0	7 left	0	15 left	5 left	0	7.5 left

TABLE III.- MOMENTS AND PRODUCT OF INERTIA

ϵ, deg	I_X, slug-ft^2	I_Y, slug-ft^2	I_Z, slug-ft^2	I_{XZ}, slug-ft^2	$\dfrac{I_X - I_Y}{mb^2}$
		Configuration A			
0	13 449	128 000	138 151	0	-1 022 $\times$ 10^{-4}
1	13 487	128 000	138 113	2 176	-1 022
2	13 601	128 000	137 999	4 350	-1 021
3	13 791	128 000	137 809	6 518	-1 019
4	14 056	128 000	137 544	8 677	-1 017
5	14 396	128 000	137 204	10 827	-1 014
		Configuration B			
0	11 709	82 654	89 237	0	-755 $\times$ 10^{-4}
1	11 733	82 654	89 213	1 353	-754
2	11 804	82 654	89 142	2 704	-754
3	11 921	82 654	89 025	4 052	-752
4	12 086	82 654	88 860	5 395	-751
5	12 298	82 654	88 648	6 731	-748
		Configuration C			
0	4 288	73 384	74 867	0	-3 536 $\times$ 10^{-4}
1	4 310	73 384	74 846	1 232	-3 534
2	4 374	73 384	74 781	2 462	-3 531
3	4 481	73 384	74 674	3 689	-3 526
4	4 631	73 384	74 524	4 911	-3 518
5	4 824	73 384	74 331	6 128	-3 508

TABLE IV.- RESULTS OF DEVELOPED-SPIN CALCULATIONS

ϵ, deg	α, deg	β, deg	$\dot{\psi}_e$, rad/sec	V_R, ft/sec	E_s	Turns for recovery
Configuration A						
0	73.8	-2.0	1.26	318	0.1308	3.44
1	74.0	-1.9	1.24	318	.1257	3.33
2	74.0	-1.9	1.21	318	.1185	3.21
3	74.1	-1.8	1.19	318	.1136	3.10
4	74.1	-1.8	1.17	317	.1093	3.02
5	74.1	-1.8	1.15	317	.1044	2.93
Configuration B*						
0	65.6 to 85.7	-25.3 to 17.6	1.69 to 2.63	341 to 343	0.4213	5.66
1	63.7 to 87.3	-25.5 to 17.3	1.59 to 2.68	344 to 346	.4007	4.10
2	61.0 to 88.5	-17.1 to 13.8	1.58 to 2.62	345 to 348	.3785	4.37
3	60.5 to 90.7	-16.4 to 15.0	1.49 to 2.61	345 to 348	.3601	3.36
4	61.9 to 92.8	-15.1 to 11.9	1.45 to 2.57	345 to 347	.3513	3.44
5	59.8 to 92.5	-14.7 to 14.5	1.39 to 2.62	345 to 348	.3396	3.54
Configuration C*						
0	83.6 to 87.2	-6.4 to 0.2	2.07	277	1.5967	6.98
1	84.5 to 87.3	-5.6 to .1	1.98	276	1.4694	6.22
2	85.1 to 87.4	-4.9 to -.3	1.91	276	1.3646	5.88
3	85.7 to 87.8	-4.3 to -.3	1.84	276	1.2642	5.66
4	85.1 to 88.2	-4.0 to -.4	1.74	276	1.1256	5.28
5	85.5 to 88.6	-3.5 to -.4	1.65	275	1.0169	5.01

*Range of oscillations given.

TABLE V.- RESULTS OF ADDITIONAL DEVELOPED-SPIN CALCULATIONS

FOR CONFIGURATION B[*]

ϵ, deg	α, deg	β, deg	$\dot{\psi}_e$, rad/sec	V_R, ft/sec	E_s	Turns for recovery
0	61.5 to 71.6	-5.9 to 0.3	1.11 to 1.41	359 to 362	0.1175	3.67
1	62.4 to 71.8	-4.7 to 0	1.11 to 1.37	359 to 361	.1135	3.64
2	62.6 to 72.5	-5.2 to 0.3	1.08 to 1.33	359 to 361	.1064	2.92
3	62.0 to 73.3	-4.9 to 0.4	1.05 to 1.35	358 to 361	.1045	2.90
4	62.2 to 74.0	-5.5 to 0.8	1.02 to 1.35	357 to 360	.1017	2.26
5	62.6 to 74.8	-5.5 to 1.1	1.00 to 1.35	357 to 360	.0995	2.29

[*]Range of oscillations given.
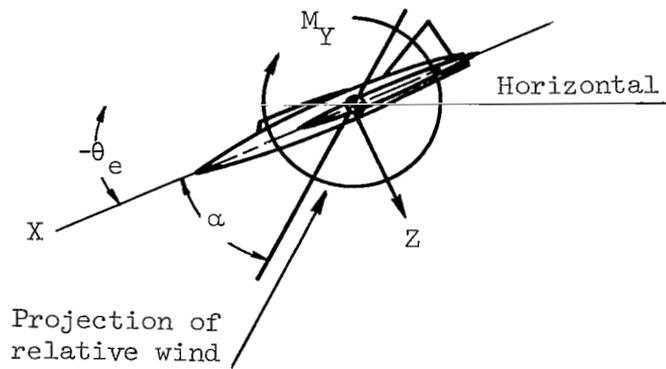
(a) ϕ_e and $\psi_e = 0$.
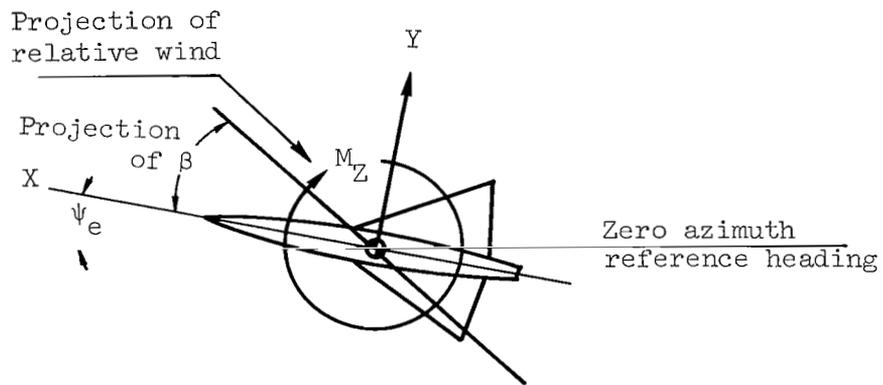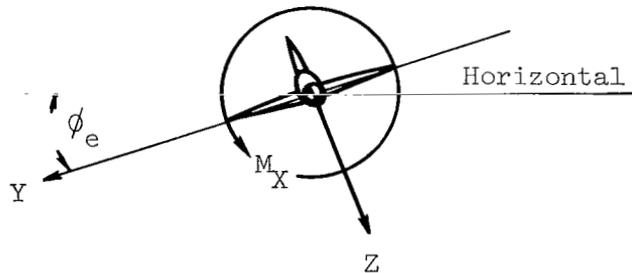
(b) θ_e and $\phi_e = 0$.

(c) θ_e and $\psi_e = 0$, and in this case $\phi = \phi_e$.

Figure 1.- Three-view sketch showing body system of axes, related angles, and positive directions of corresponding forces and moments.
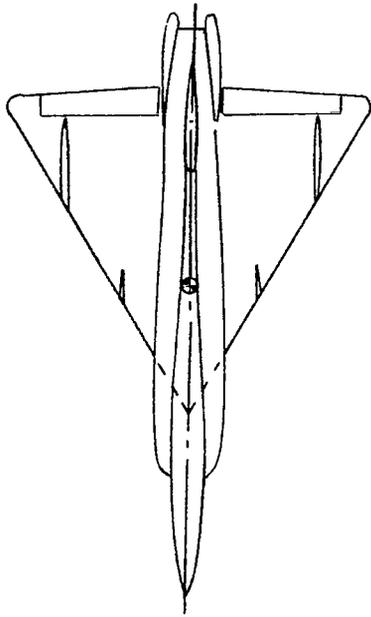
Configuration A
(delta-wing fighter)
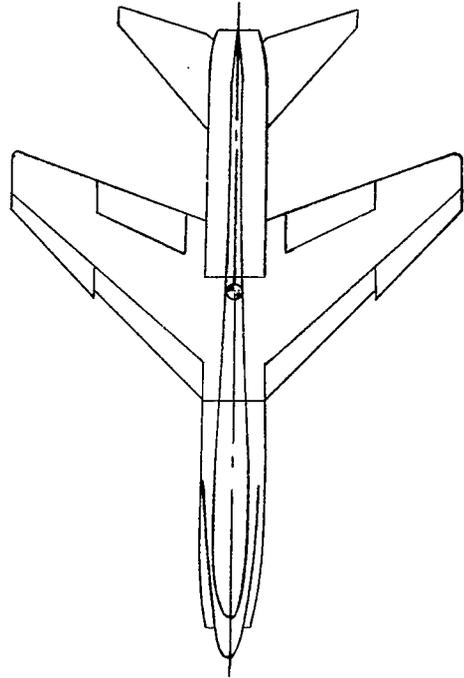
Configuration B
(swept-wing fighter)
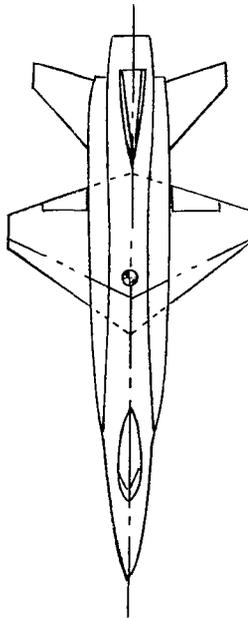
Configuration C
(stub-wing vehicle)

Figure 2.- Planview of three configurations investigated.
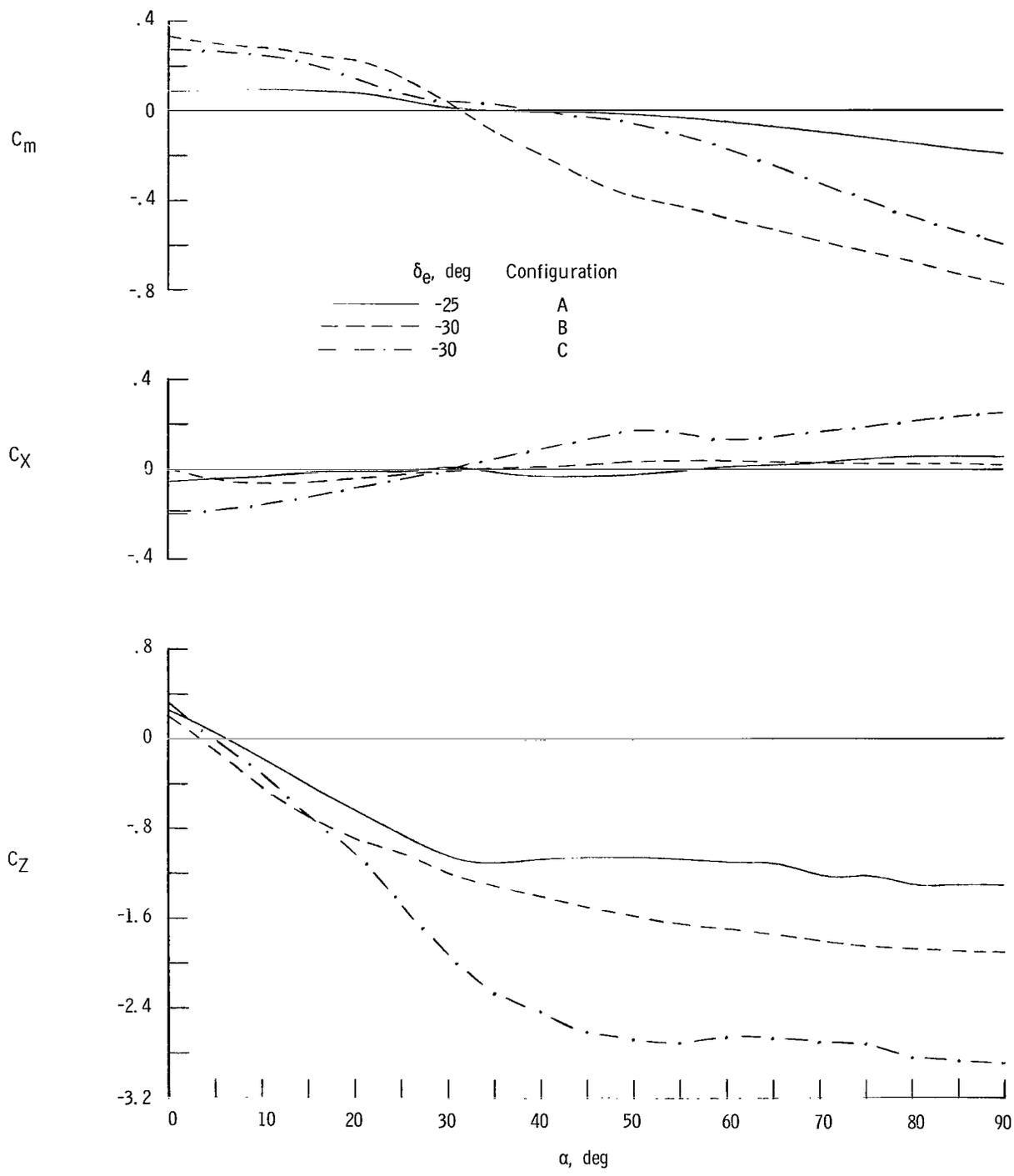
Figure 3.- Variation of static longitudinal stability characteristics. Measurements are referred to 30-, 33-, and 19-percent mean-aerodynamic-chord positions for configurations A, B, and C, respectively.
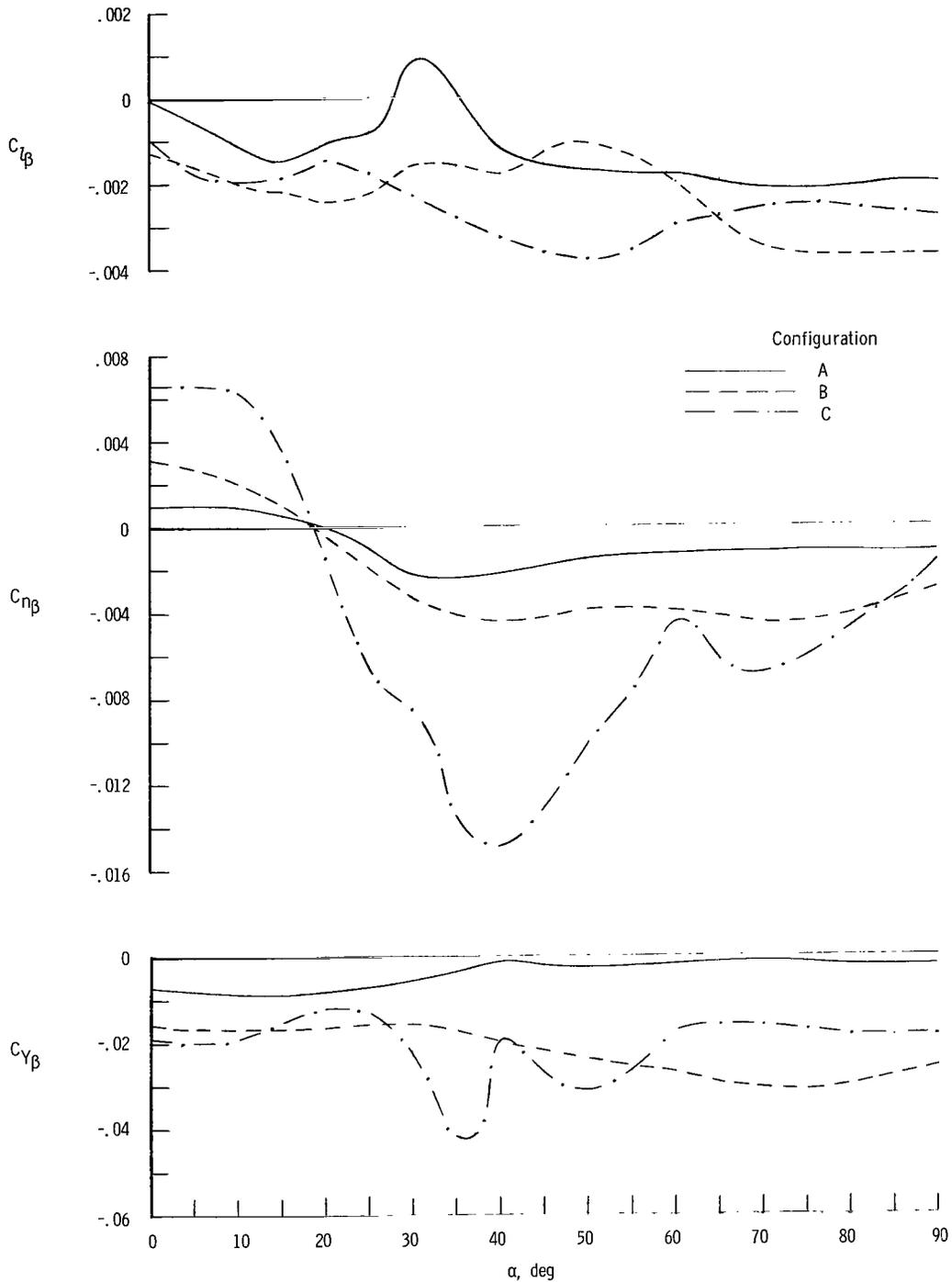
Figure 4.- Variation of static lateral and directional stability derivatives with angle of attack. Measurements are referred to the 30-, 33-, and 19-percent mean-aerodynamic-chord positions for configurations A, B, and C, respectively.
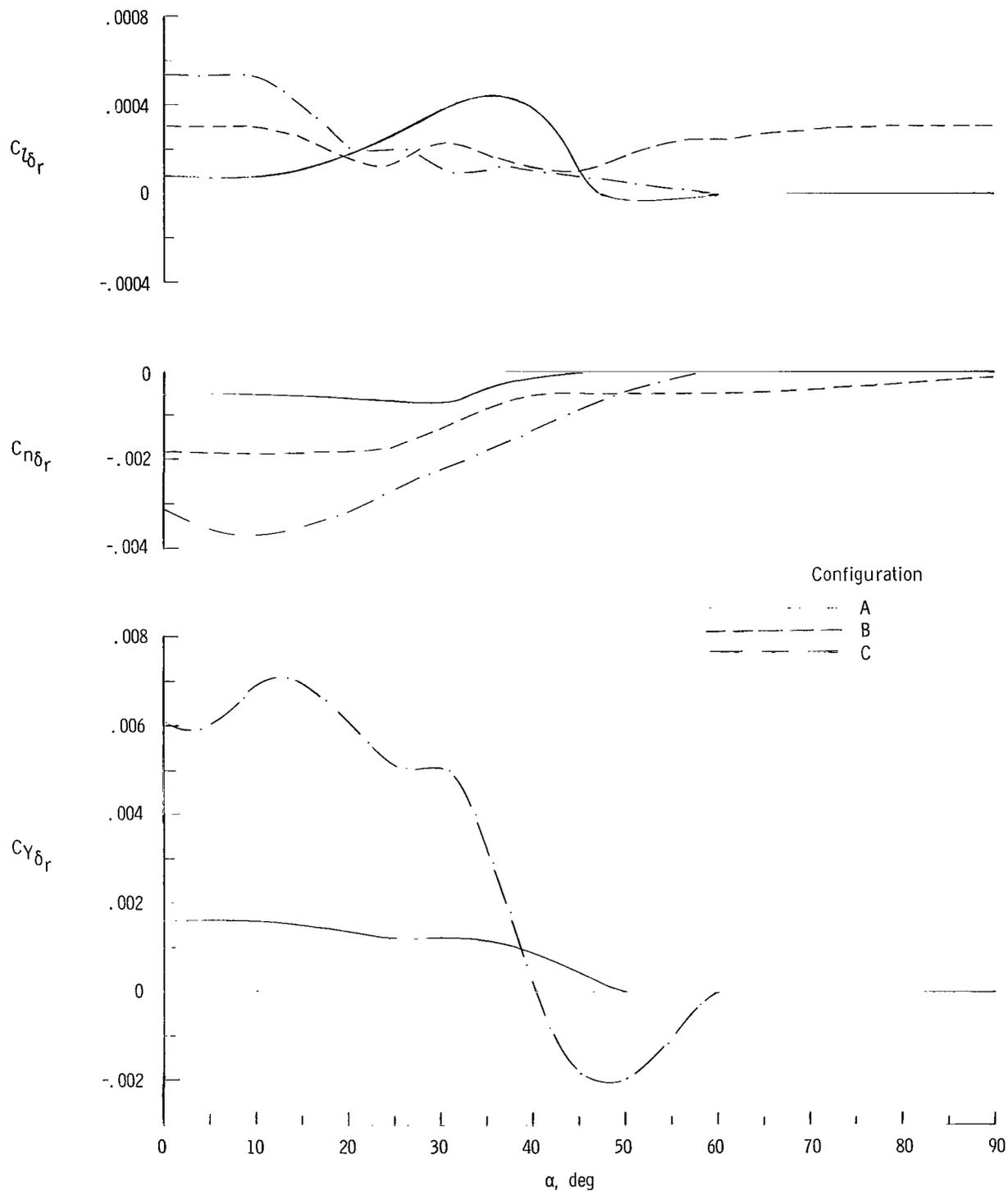
Figure 5.- Variation of rudder effectiveness parameters with angle of attack.
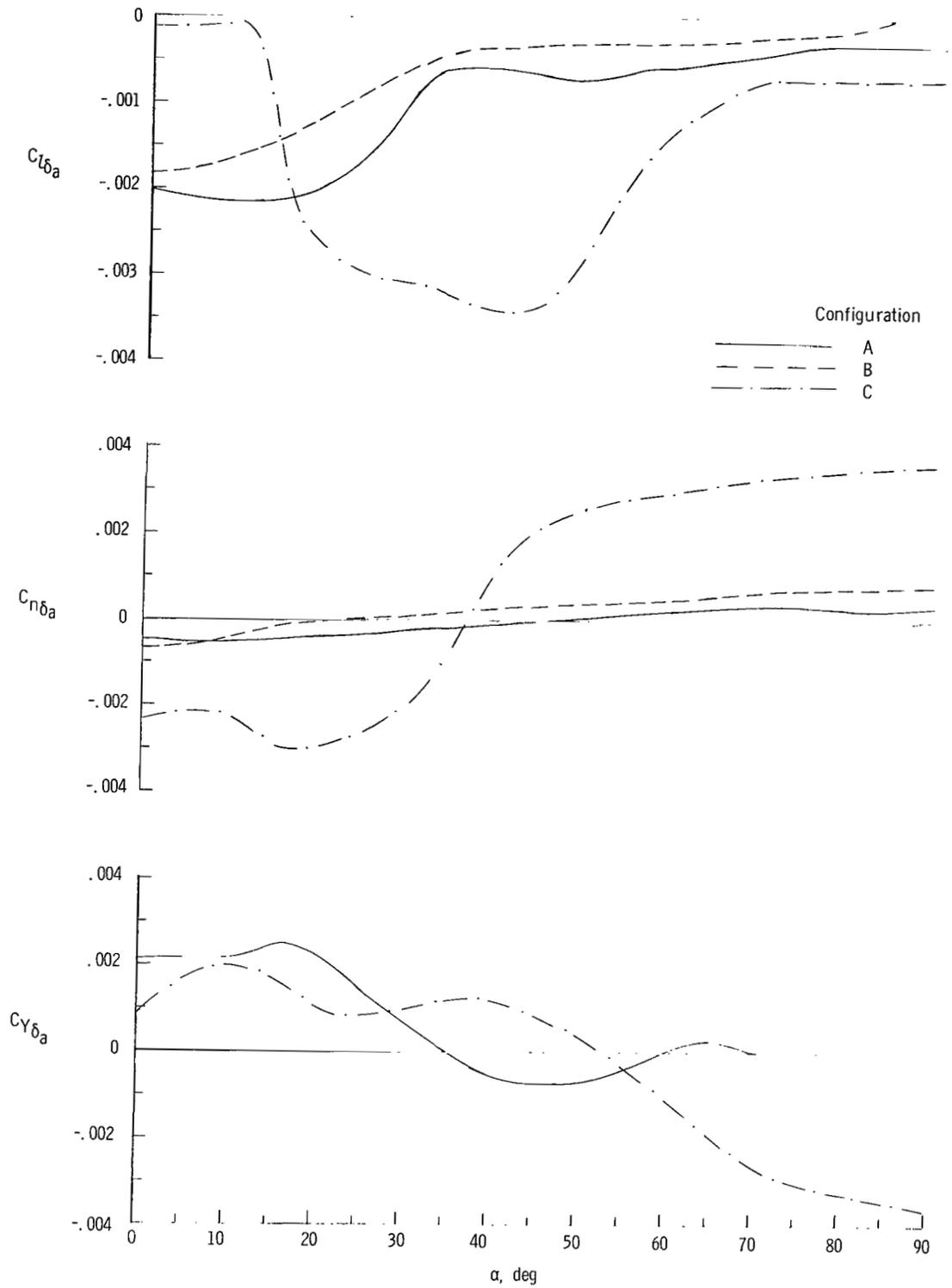
Figure 6.- Variation of aileron effectiveness parameters with angle of attack.
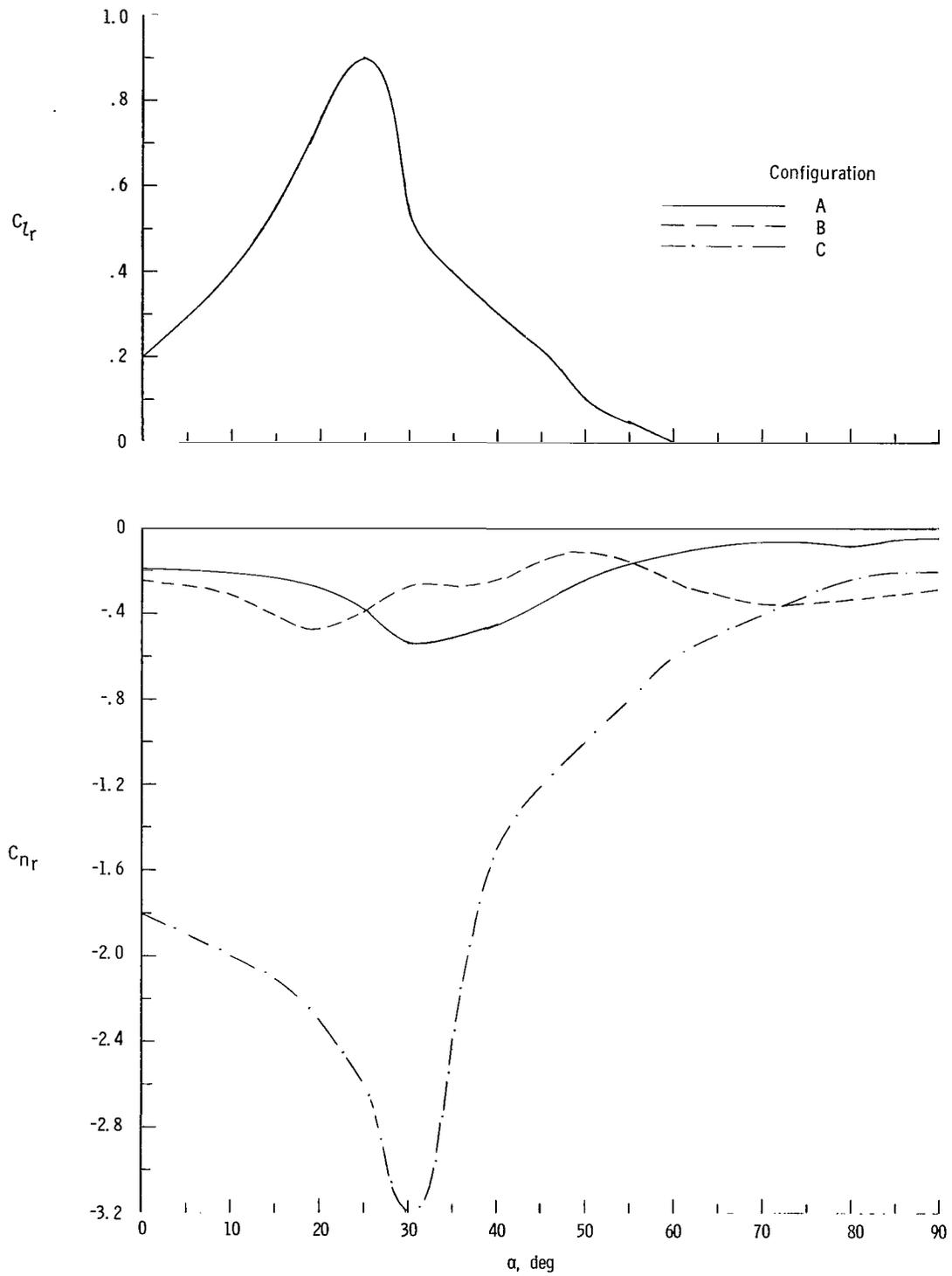
Figure 7.- Variation of C_{l_r} and C_{n_r} with angle of attack.
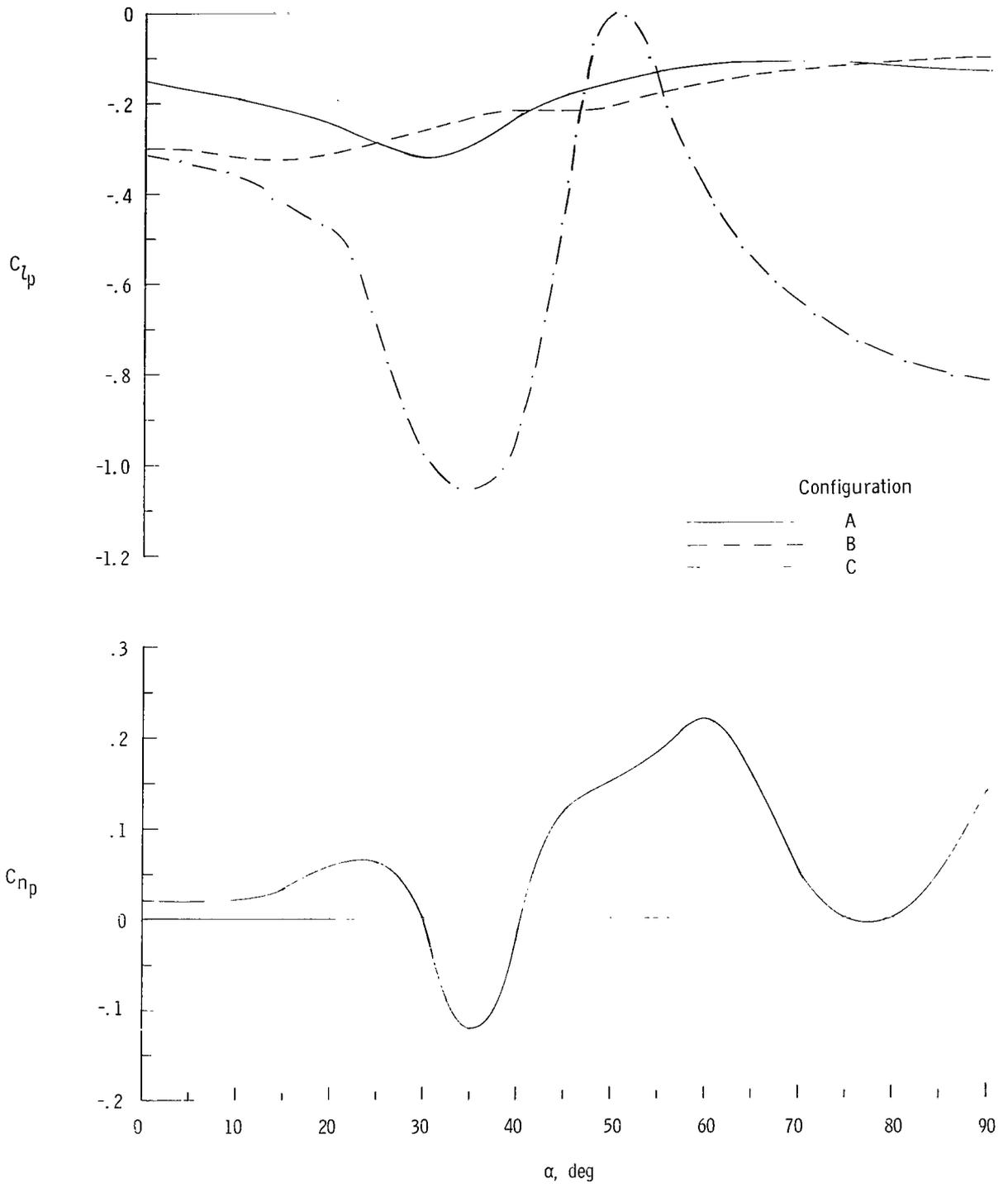
Figure 8.- Variation of C_{l_p} and C_{n_p} with angle of attack.
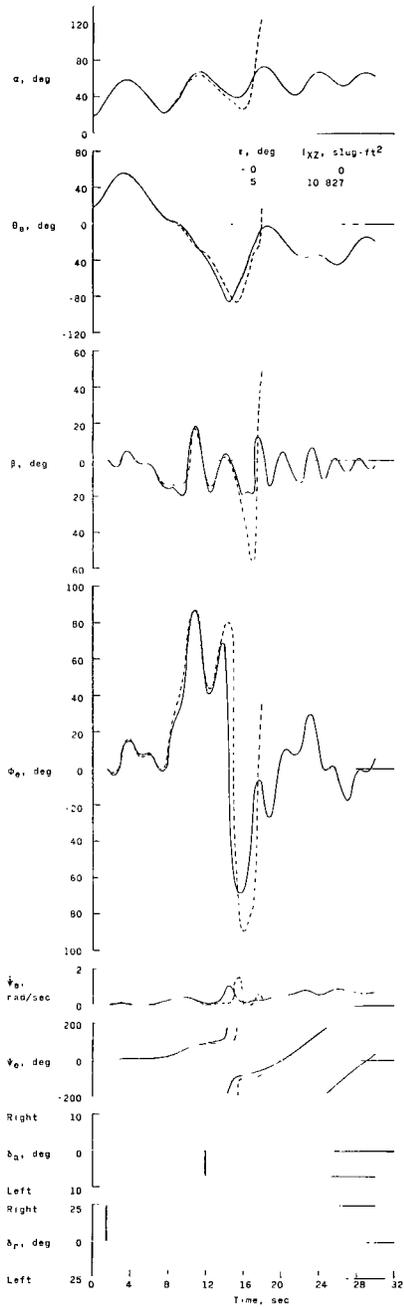
Figure 9.- Calculated spin-entry motions for configuration A. $\delta_e = -25°$.
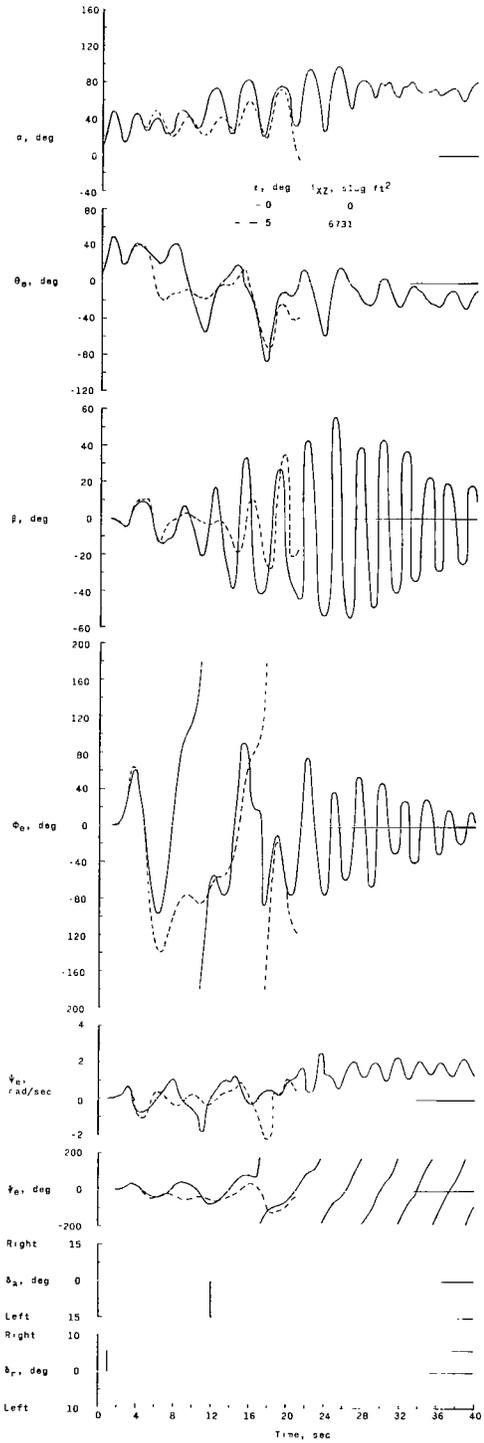
Figure 10.- Calculated spin-entry motions for configuration B. $\delta_e = -30°$.
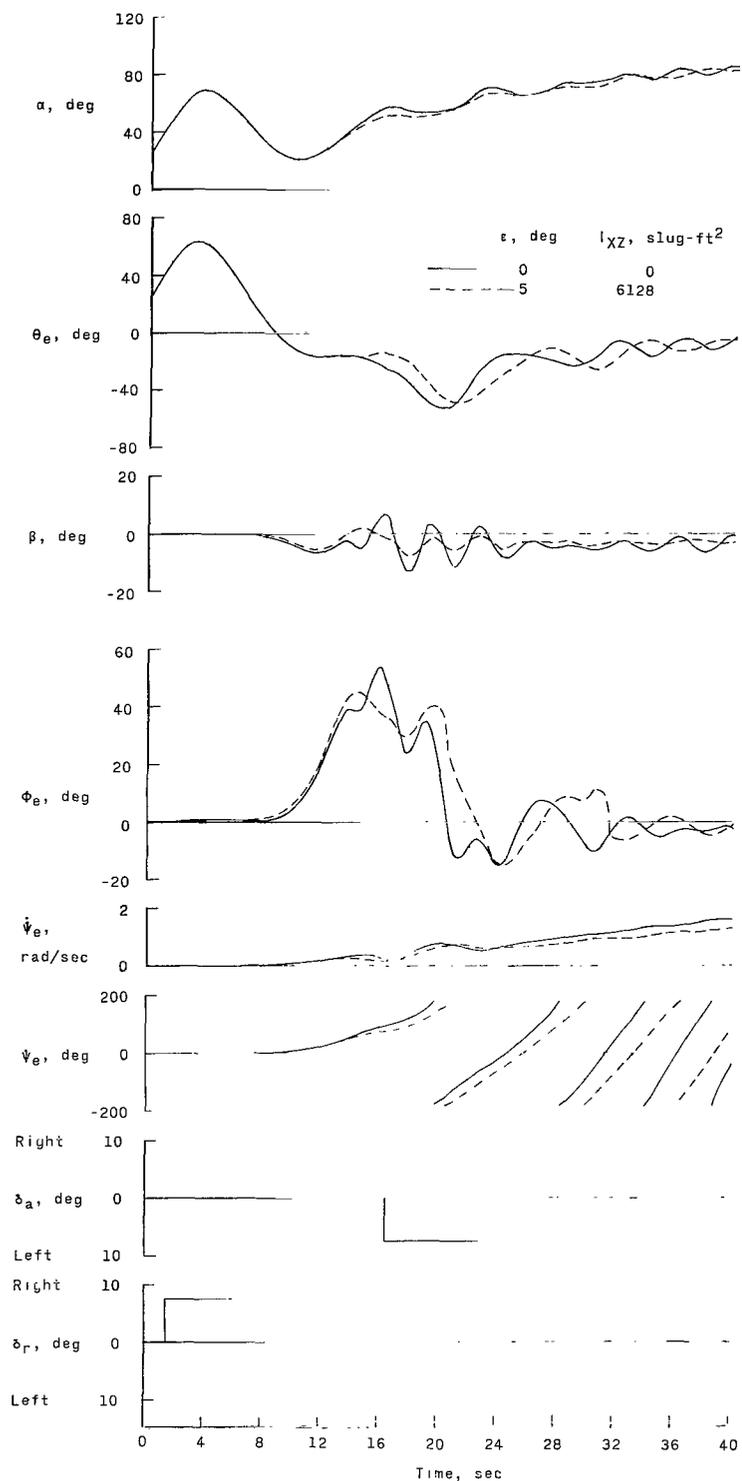
Figure 11.- Calculated spin-entry motions for configuration C. $\delta_e = -30°$.
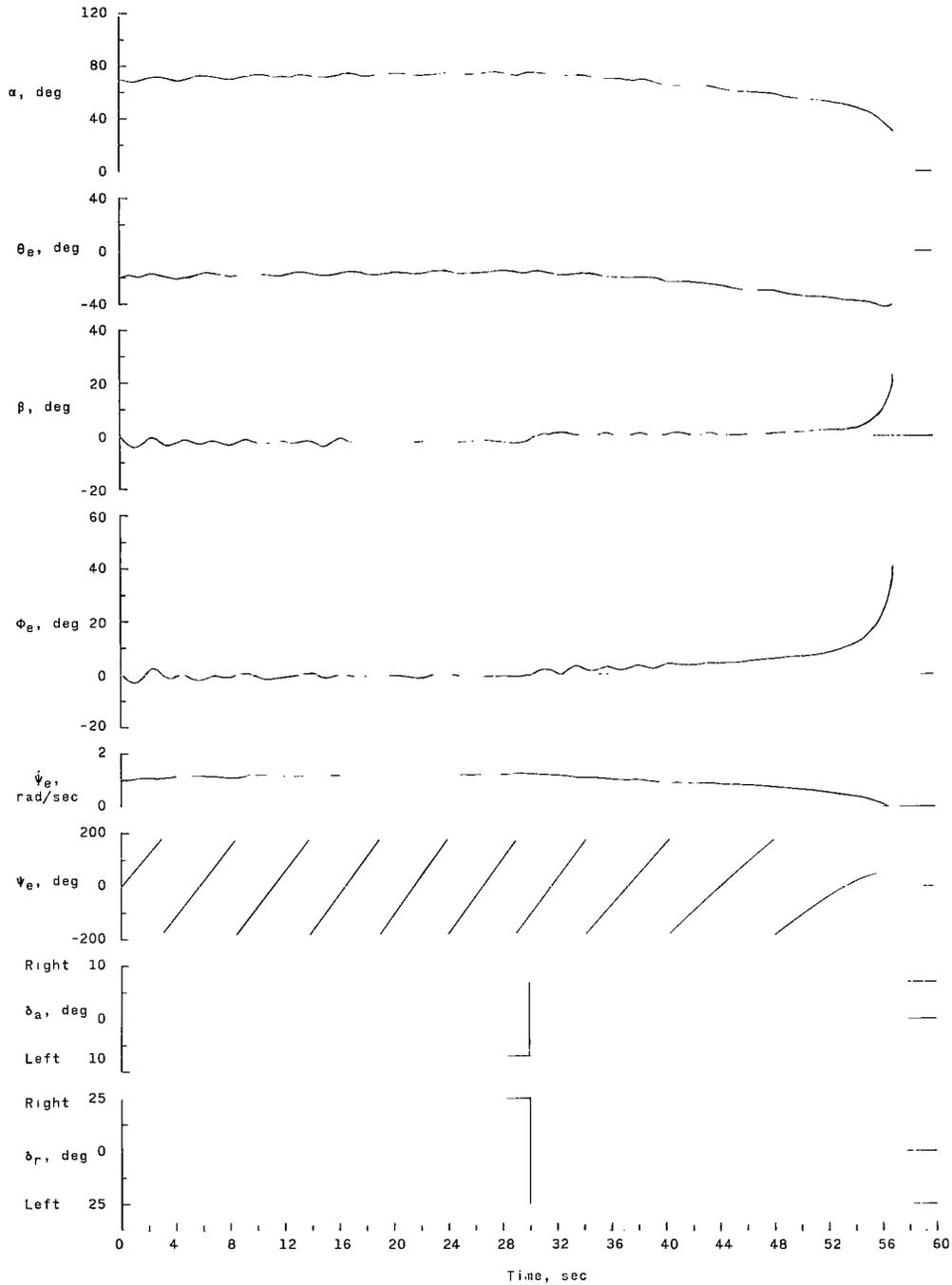
(a) $\epsilon = 0°$; $I_{XZ} = 0$ slug-ft^2.

Figure 12.- Calculated developed-spin and spin-recovery motions for configuration A. $\delta_e = -25°$.
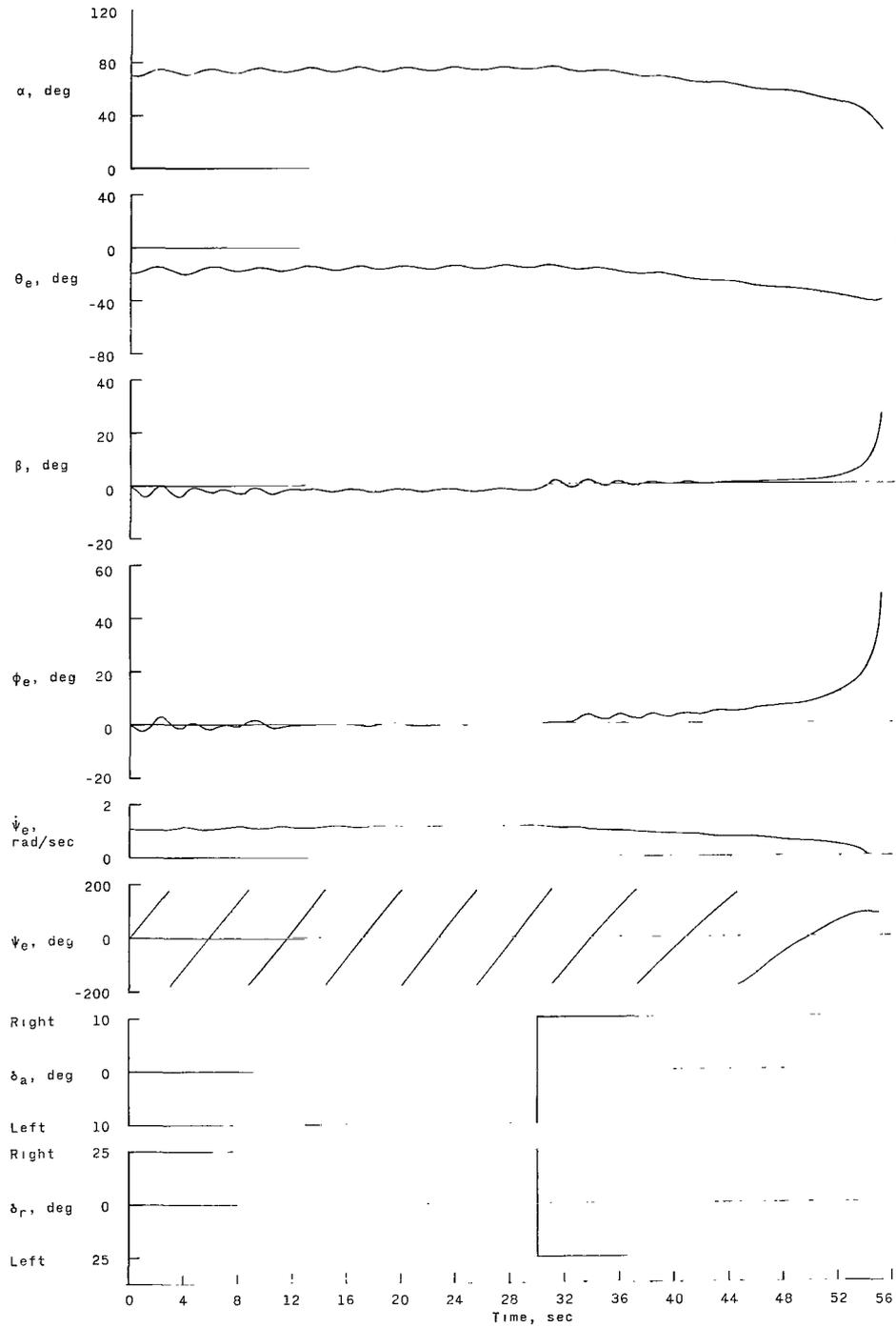
(b) $\epsilon = 5°$; $I_{XZ} = 10\ 827$ slug-ft^2.

Figure 12.- Concluded.
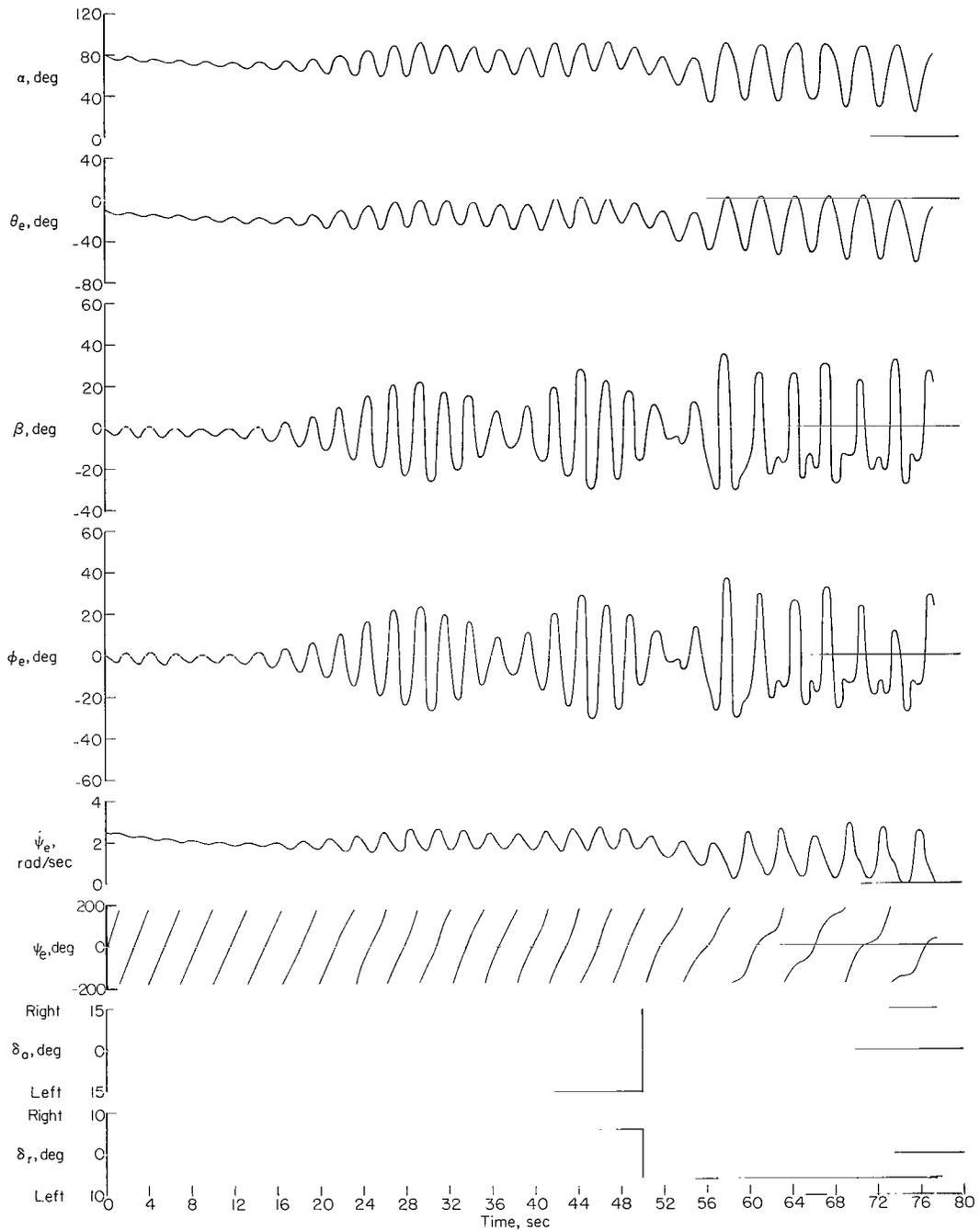
(a) $\epsilon = 0°$; $I_{XZ} = 0$ slug-ft^2.

Figure 13.- Calculated developed-spin and spin-recovery motions for configuration B. $\delta_e = -30°$.
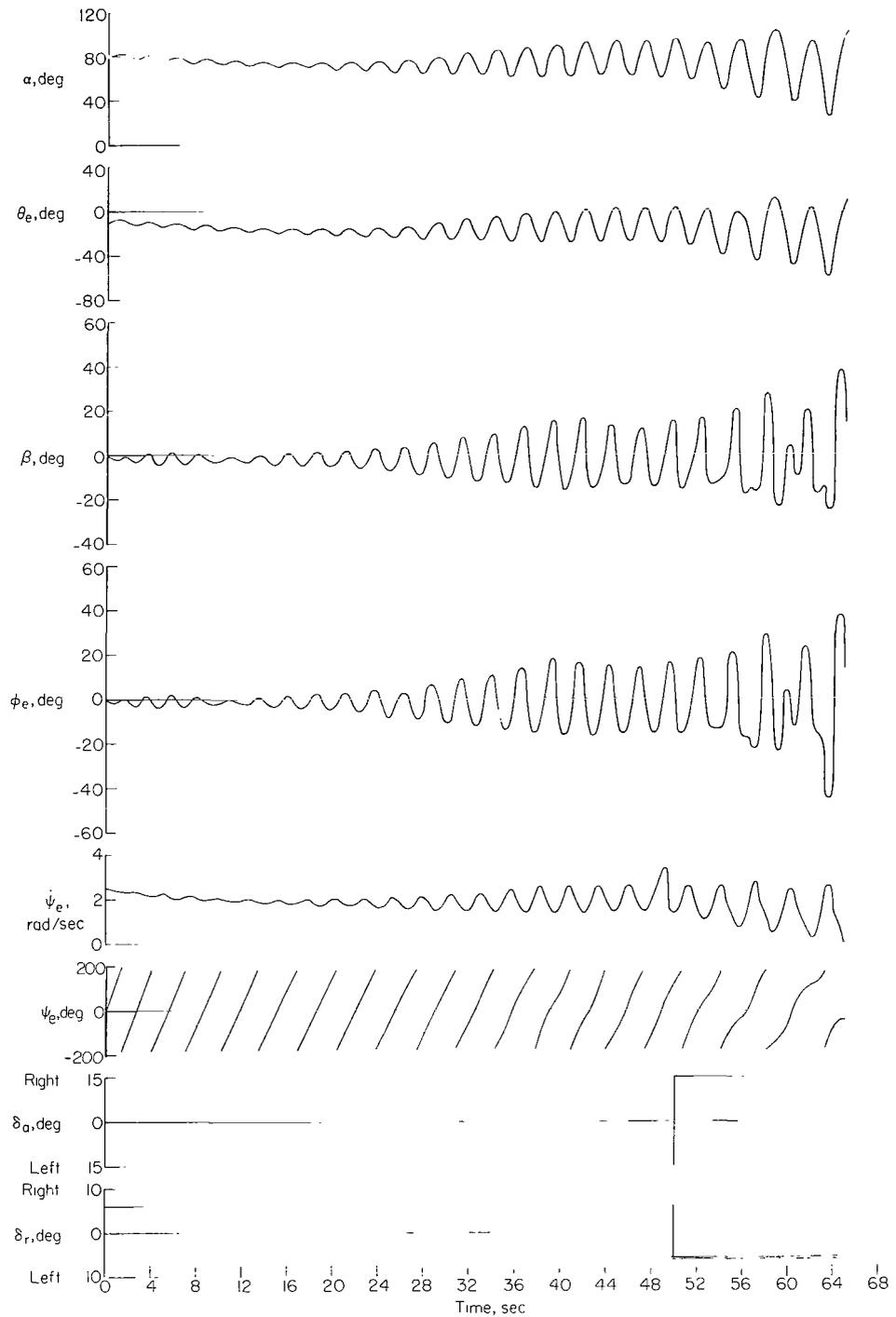
(b) $\epsilon = 5^{\circ}$; $I_{XZ} = 6\ 731$ slug-ft^2.

Figure 13.- Concluded.
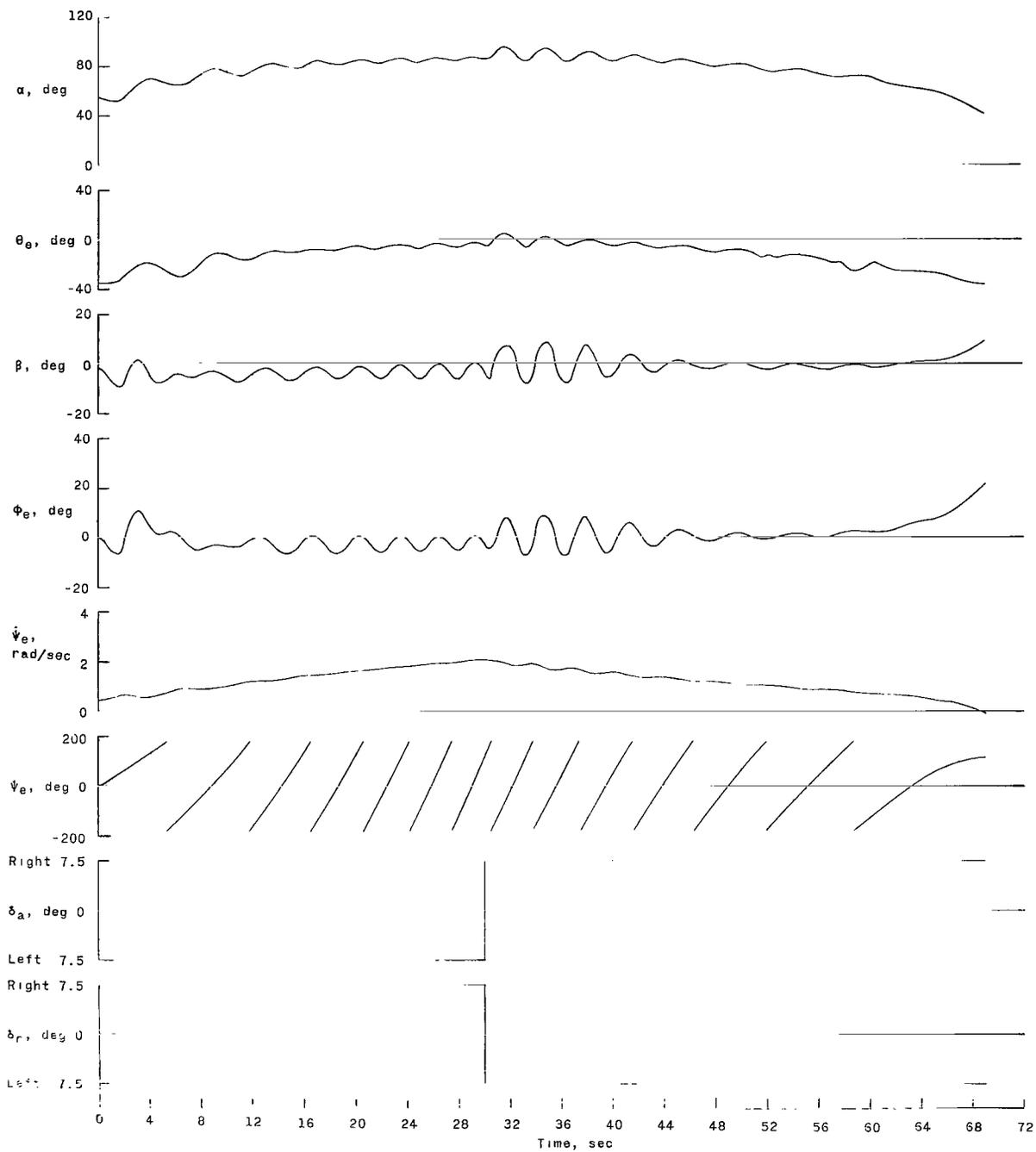
(a) $\epsilon = 0°$; $I_{XZ} = 0$ slug-ft^2.

Figure 14.- Calculated developed-spin and spin-recovery motions for configuration C.
$\delta_e = -30°$.
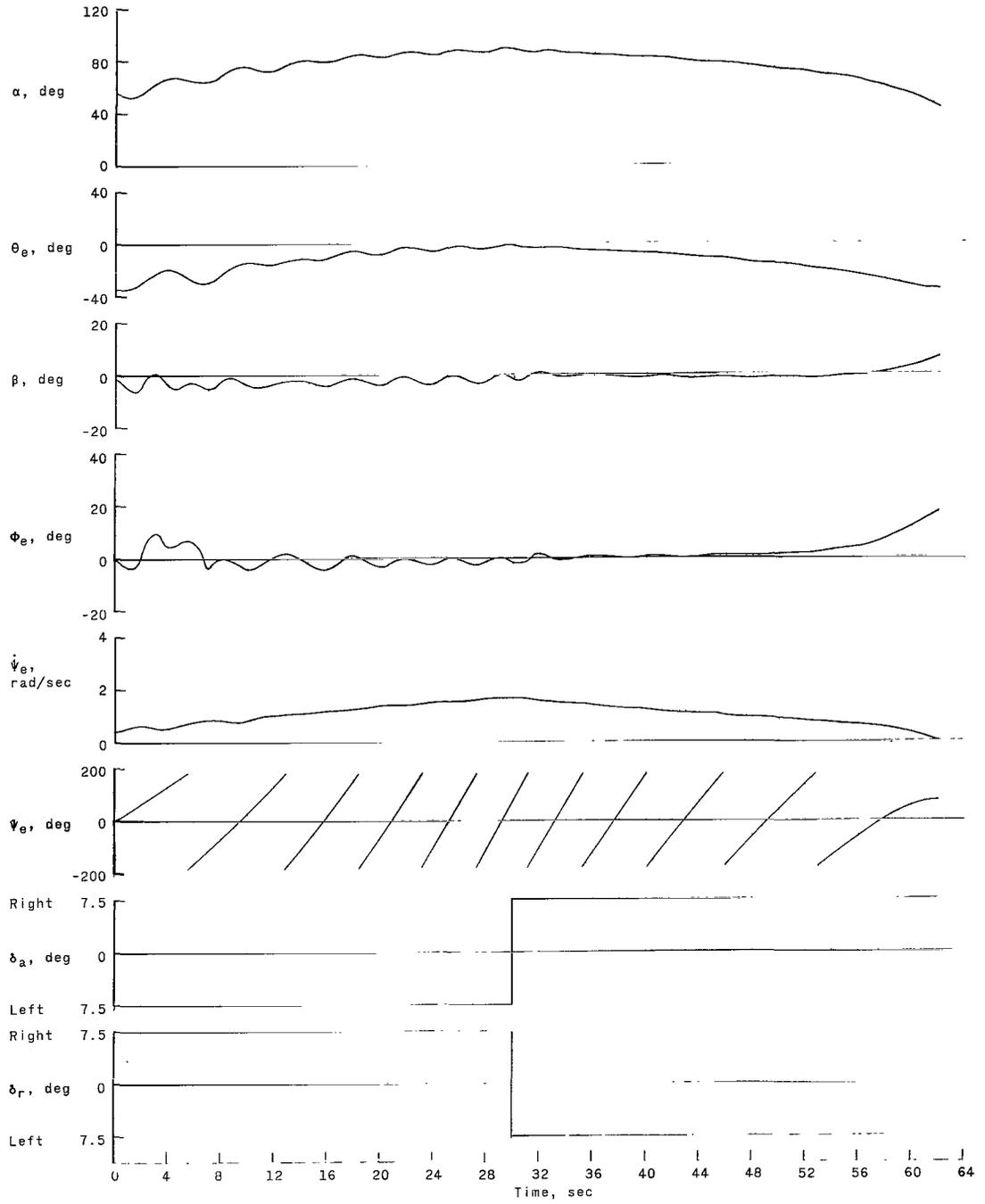
(b) $\epsilon = 5^\circ$; $I_{XZ} = 6\ 128$ slug-ft^2.

Figure 14.- Concluded.
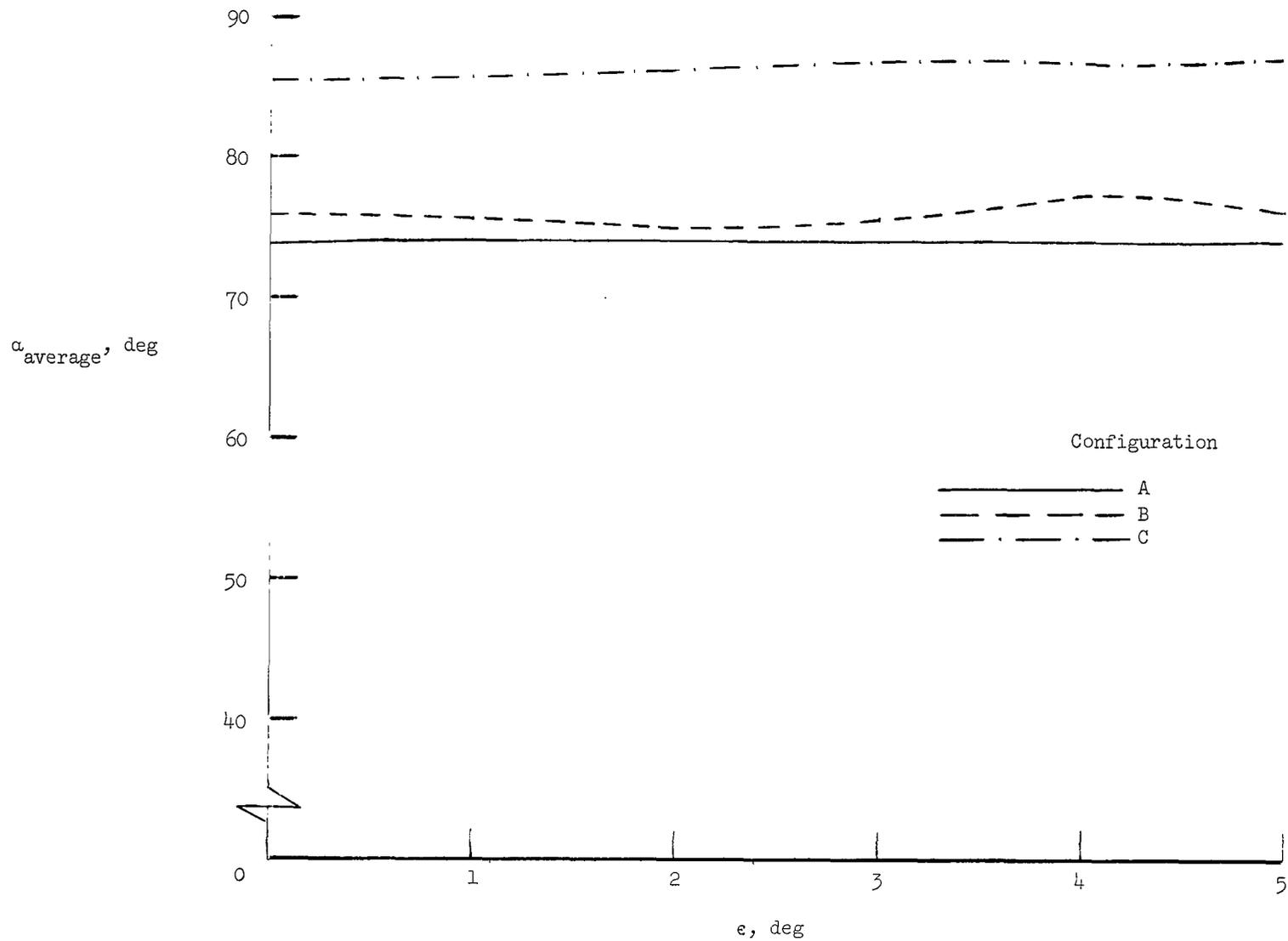
Figure 15.- Variation of developed-spin average angle of attack with ε for all configurations.
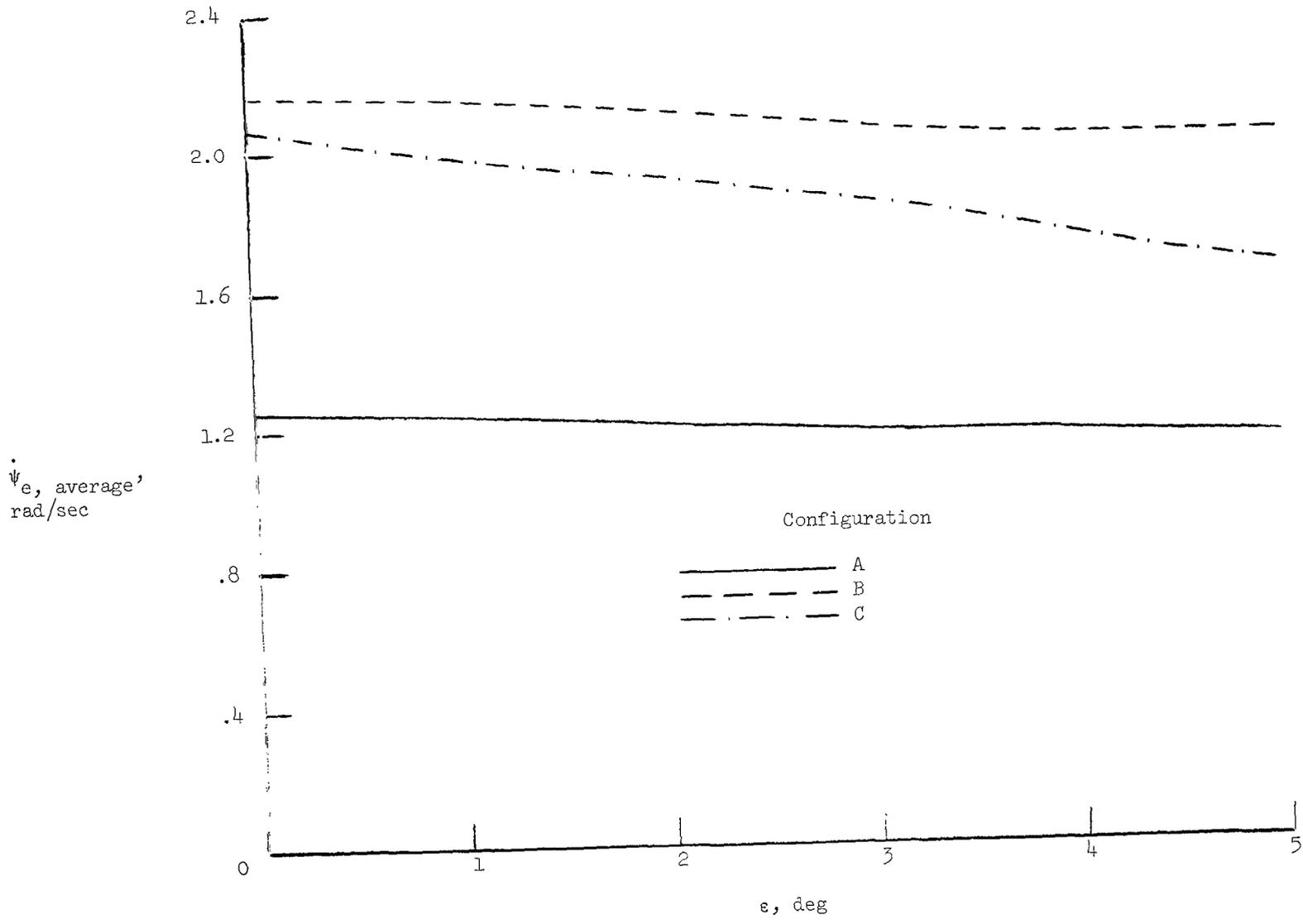
Figure 16.- Variation of developed-spin average rate of rotation with ε for all configurations.
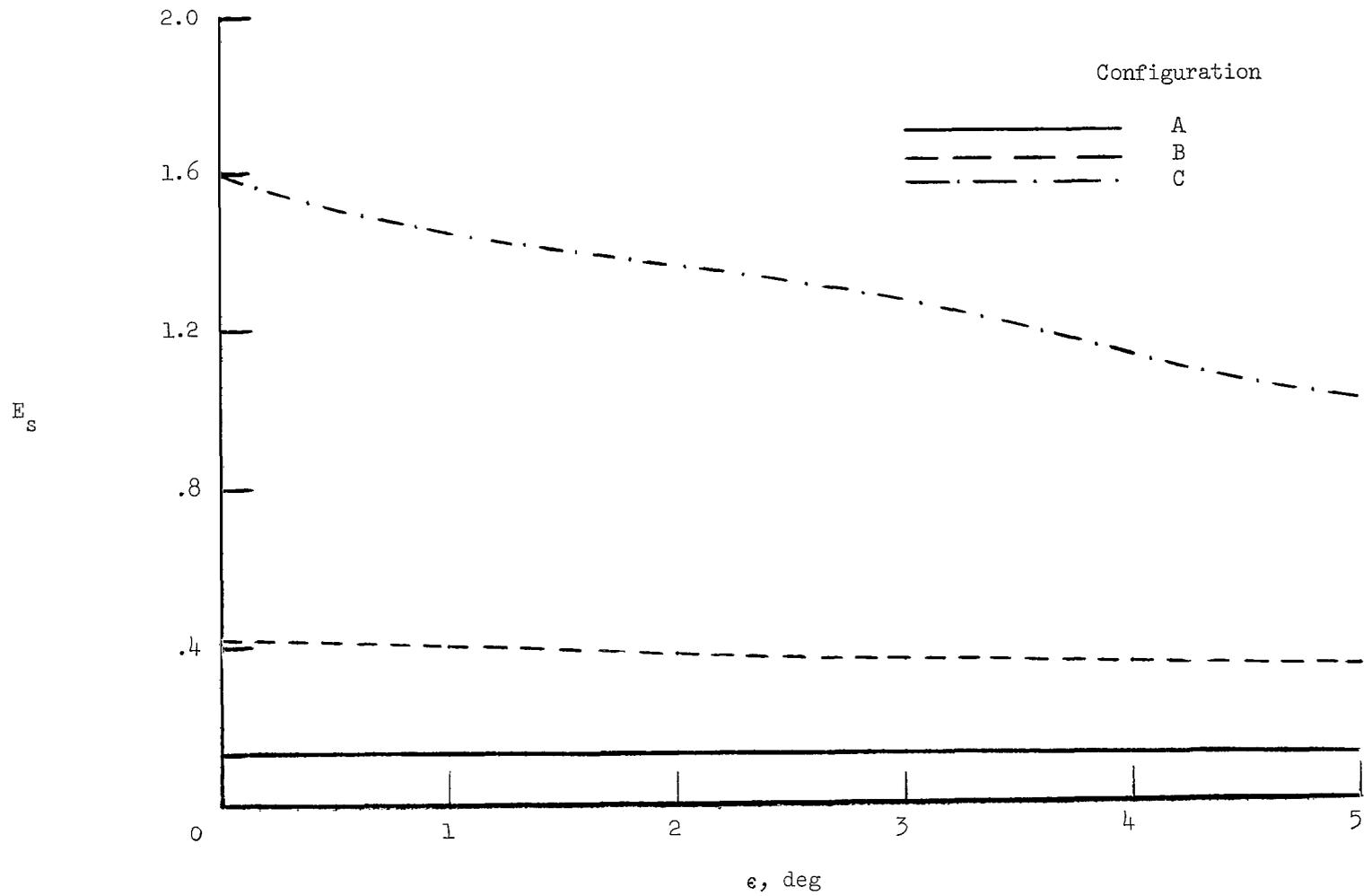
Figure 17.- Variation of spin-energy factor E_s with ϵ for all configurations.
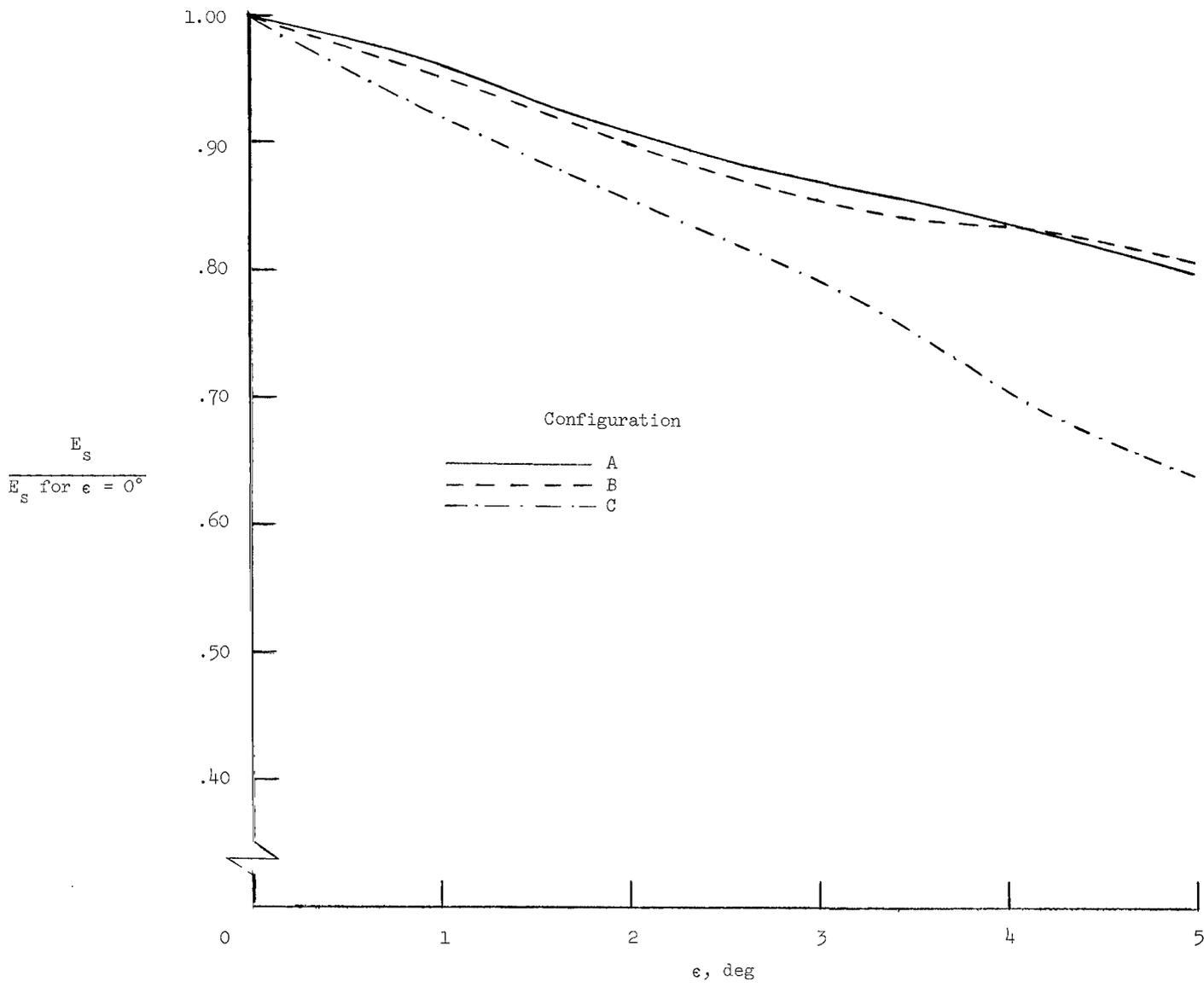
Figure 18.- Variation of $\dfrac{E_S}{E_S \text{ for } \epsilon = 0^O}$ with ϵ for all configurations.
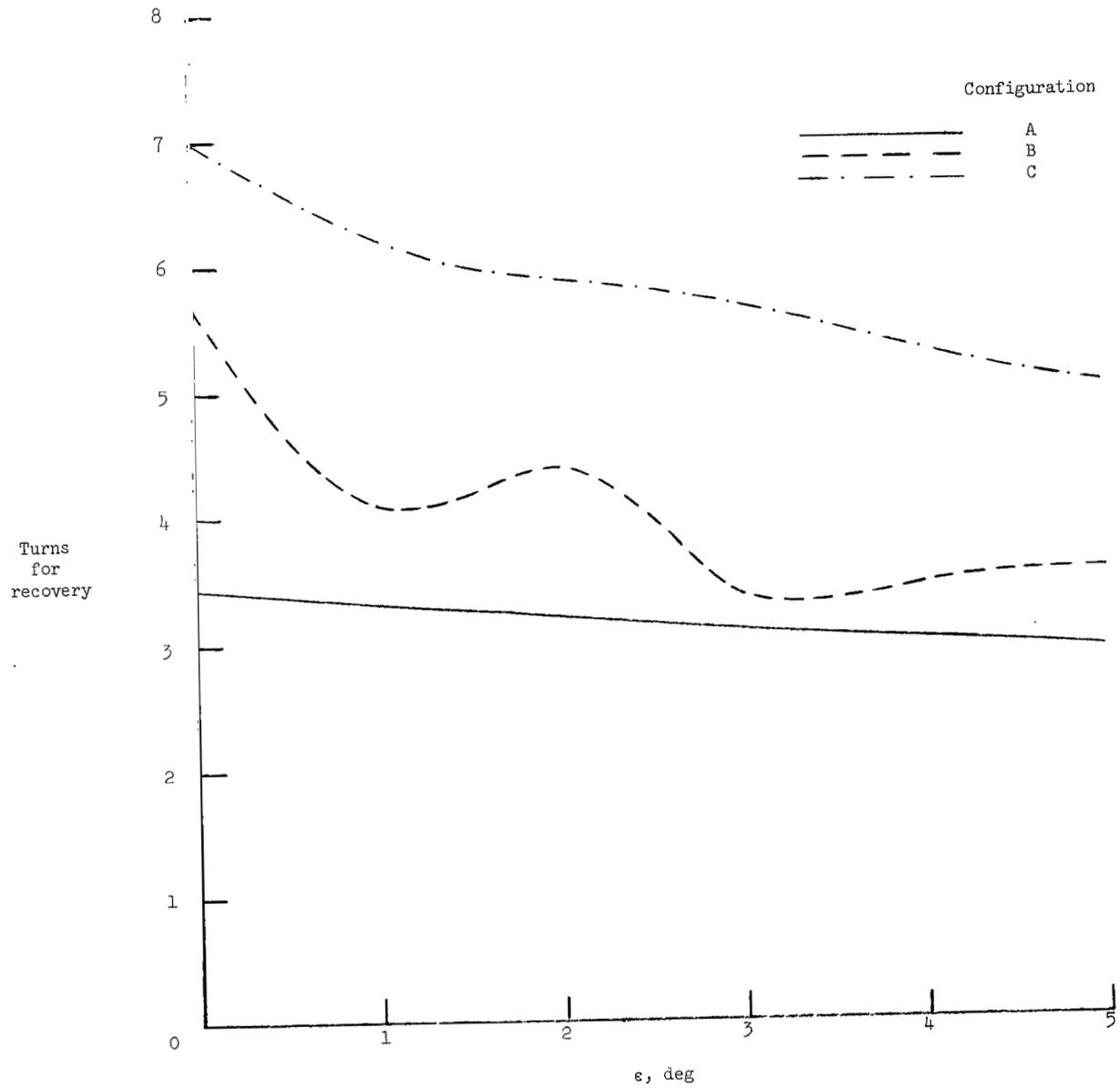
Figure 19.- Variation of turns required for recovery with ε for all configurations.
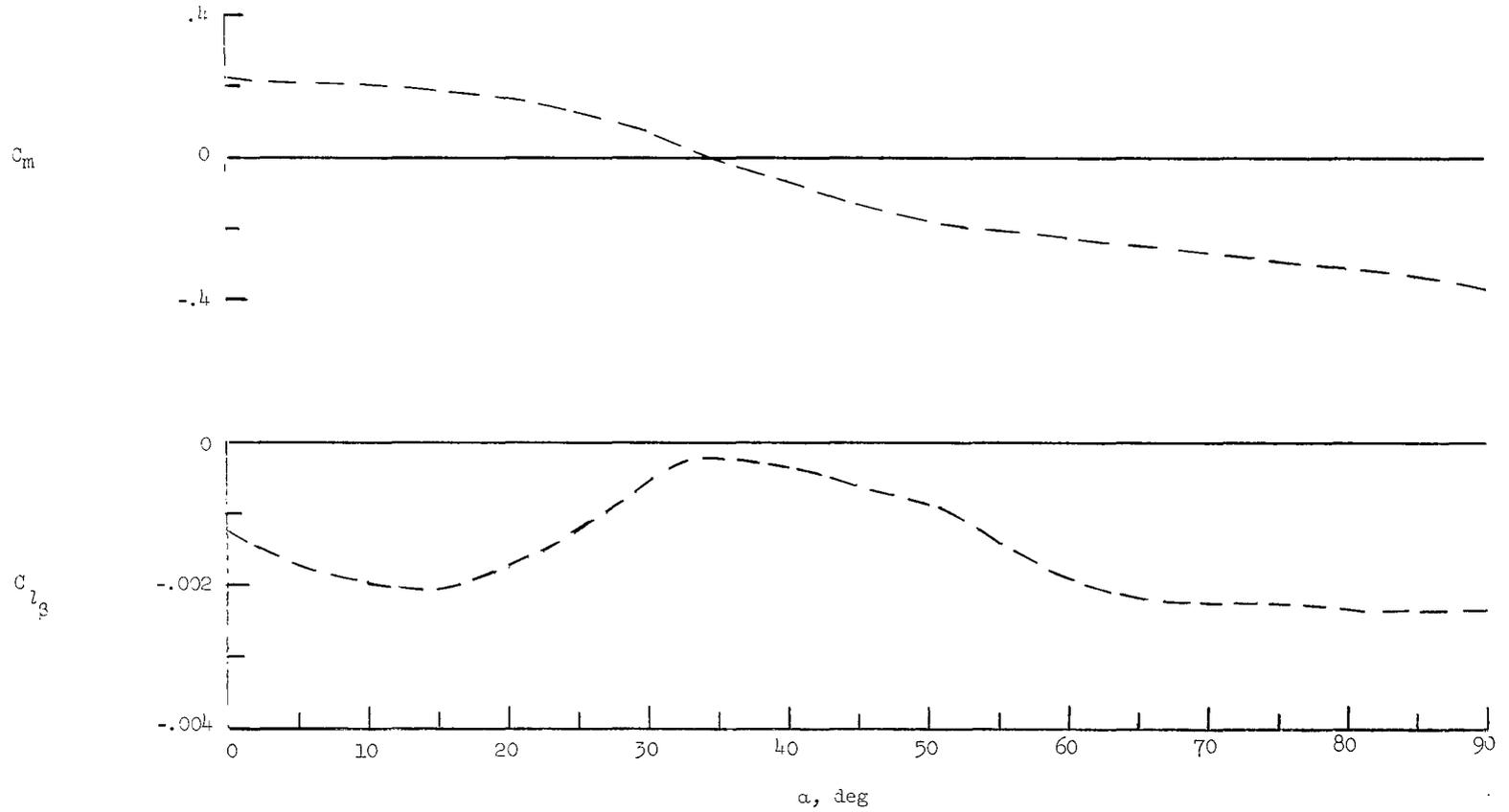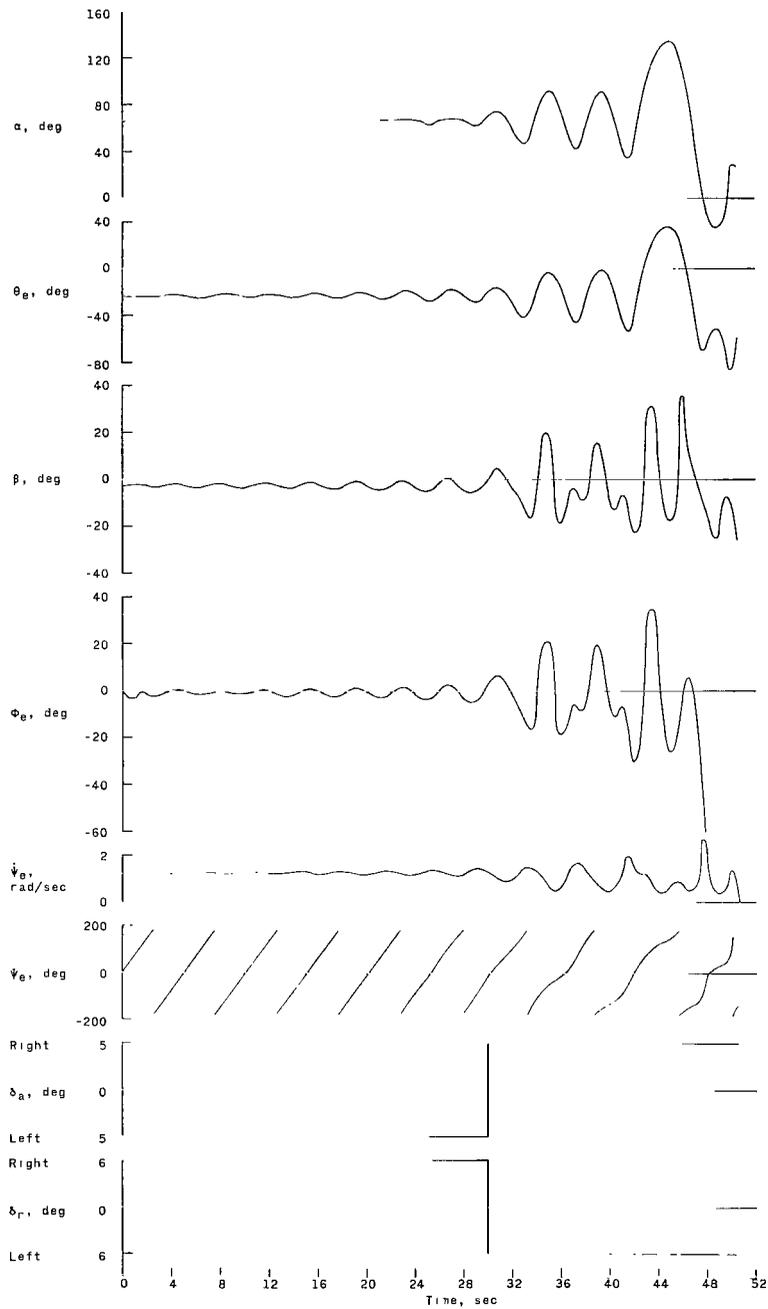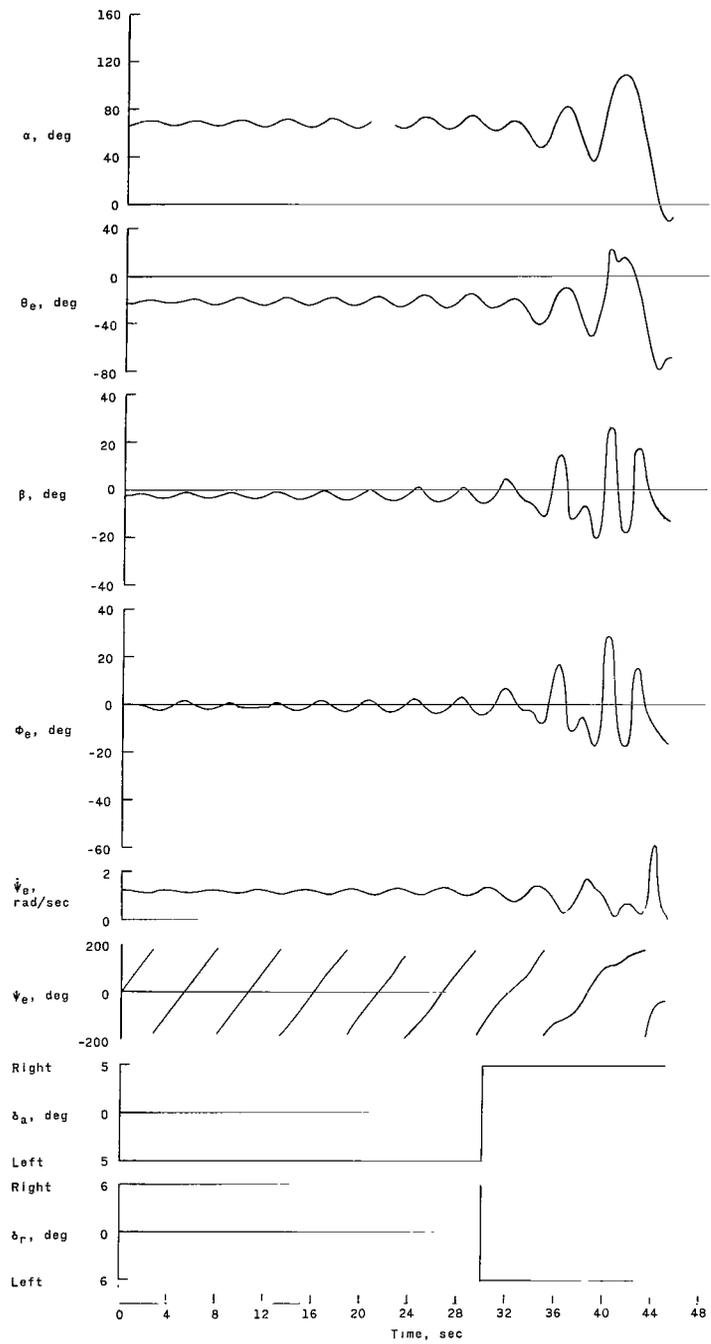
Figure 20.- Estimated variation of C_m and C_{l_β} coefficients with α, used for additional calculations for configuration B. δ_e = -20°.

(a) $\epsilon = 0^o$; $I_{XZ} = 0$ slug-ft^2.

Figure 21.- Additional calculated developed-spin and spin-recovery motions for configuration B. Estimated values of C_m and C_{l_β} of figure 20 used. $\delta_e = -20^o$.

(b) $\epsilon = 5^{\circ}$; $I_{XZ} = 6\ 731$ slug-ft^2.
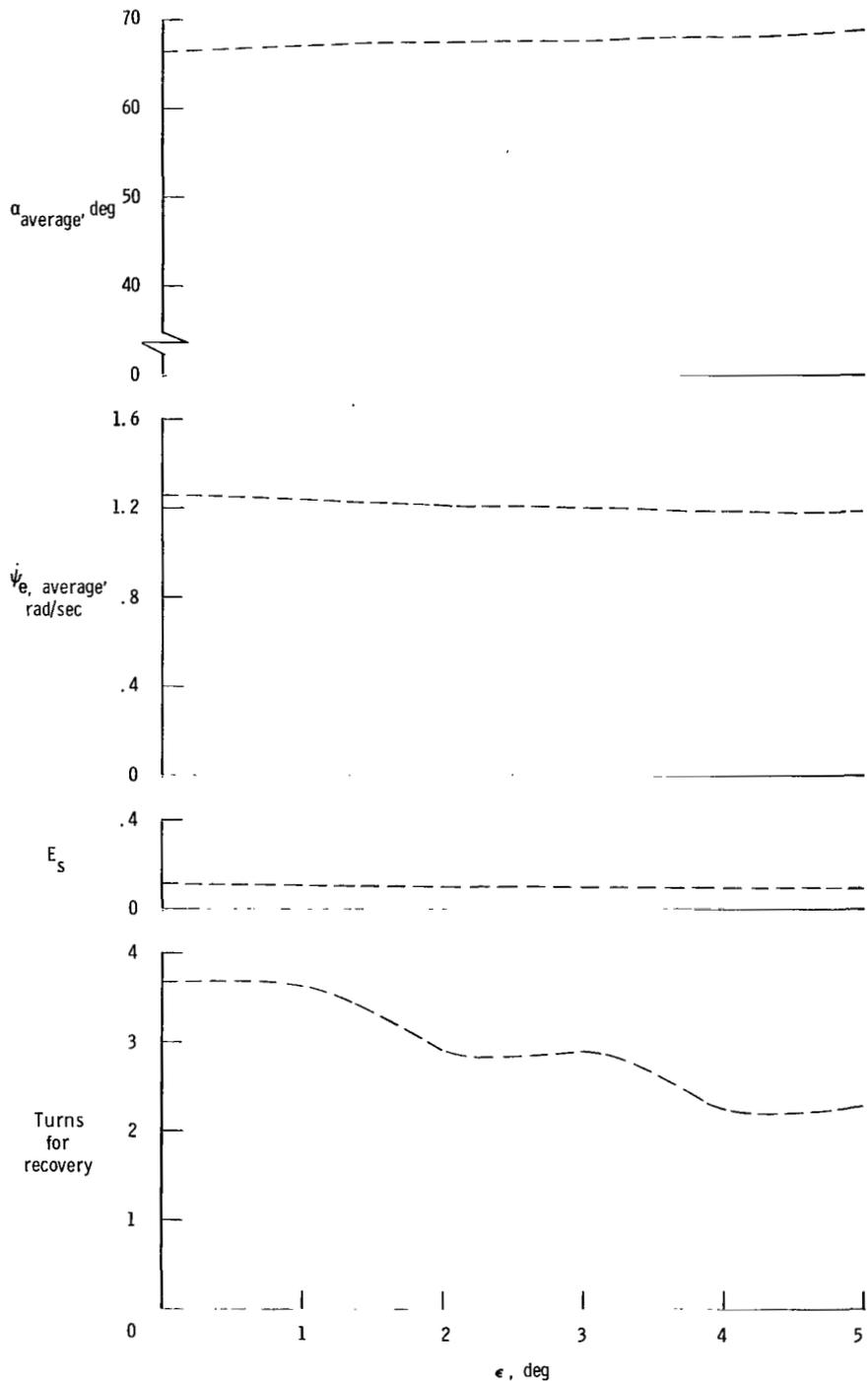
Figure 21.- Concluded.

Figure 22.- Variation of developed-spin average angle of attack, average rate of rotation, spin-energy factor, and turns required for recovery with ϵ for additional calculations for configuration B.

"The aeronautical and space activities of the United States shall be conducted so as to contribute . . . to the expansion of human knowledge of phenomena in the atmosphere and space. The Administration shall provide for the widest practicable and appropriate dissemination of information concerning its activities and the results thereof."

—NATIONAL AERONAUTICS AND SPACE ACT OF 1958

NASA SCIENTIFIC AND TECHNICAL PUBLICATIONS

TECHNICAL REPORTS: Scientific and technical information considered important, complete, and a lasting contribution to existing knowledge.

TECHNICAL NOTES: Information less broad in scope but nevertheless of importance as a contribution to existing knowledge.

TECHNICAL MEMORANDUMS: Information receiving limited distribution because of preliminary data, security classification, or other reasons.

CONTRACTOR REPORTS: Technical information generated in connection with a NASA contract or grant and released under NASA auspices.

TECHNICAL TRANSLATIONS: Information published in a foreign language considered to merit NASA distribution in English.

TECHNICAL REPRINTS: Information derived from NASA activities and initially published in the form of journal articles.

SPECIAL PUBLICATIONS: Information derived from or of value to NASA activities but not necessarily reporting the results of individual NASA-programmed scientific efforts. Publications include conference proceedings, monographs, data compilations, handbooks, sourcebooks, and special bibliographies.

Details on the availability of these publications may be obtained from:

SCIENTIFIC AND TECHNICAL INFORMATION DIVISION

NATIONAL AERONAUTICS AND SPACE ADMINISTRATION

Washington, D.C. 20546